

Electrolyte Design Strategies to Construct Stable Cathode-Electrolyte Interphases for High-Voltage Sodium-Ion Batteries

Kunchen Xie, Yuchen Ji,* Luyi Yang,* and Feng Pan*

Elevating the working voltage of sodium-ion batteries is crucial for expanding their application scenarios. However, as the operating voltage of these batteries increases, the interfacial stability of existing electrolytes becomes inadequate to meet the demands of high-voltage cathode materials. Along with the interaction with cathode interface, electrolyte trends to be decomposed forming an interphase between the cathode and electrolyte, which plays an essential role in the performance of batteries. This review systematically focuses on the reconstruction of cathode-electrolyte interphase maintaining the interfacial stability via various strategies at high voltage range. The state-of-the-art characterization techniques and modeling approaches associated with cathode-electrolyte interphase are also discussed. From the perspective of electrolyte design, the interphase reconstruction strategies focus on solvent molecule manipulation, solute ion manipulation, and the regulation of solvation-ion interaction. By summarizing strategies for constructing a stable CEI on the cathode, this review aims to provide new insights into achieving high-voltage sodium-ion batteries.

1. Introduction

Over the last few decades, lithium-ion batteries (LIBs) have undergone significant development, driven by the expanding market of portable electronic devices and electric vehicles. This rapid development has resulted in soaring prices for upstream process materials for LIBs (e.g., Li₂CO₃) and the excessive consumption of lithium resources. Thus, the ability of existing lithium resources to meet the growing demand for LIBs applications in the coming decades remains uncertain. In this scenario, it is essential to explore alternative energy storage system based on low-cost and sustainable resources. As another element in the same group of the periodic table, sodium (Na) stands out as one of the most promising alternatives to lithium (Li) due to its significantly greater abundance – constituting 2.6% of the Earth's

K. Xie, Y. Ji, L. Yang, F. Pan School of Advanced Materials Peking University Shenzhen Graduate School Shenzhen 518055, P. R. China E-mail: yuchenji@pku.edu.cn; yangly@pkusz.edu.cn; panfeng@pkusz.edu.cn

The ORCID identification number(s) for the author(s) of this article can be found under https://doi.org/10.1002/aenm.202405301

DOI: 10.1002/aenm.202405301

crust compared to just 0.0017% for Li.^[2] Therefore, developing sodium-ion batteries (SIBs) to serve as a backup strategy for LIBs holds significant strategic importance.

As a crucial metric for determining battery performance, energy density is primarily influenced by the specific capacity of the electrode and the average operating voltage of the battery. Limited by the higher atomic weight (23 g mol⁻¹ vs) and the higher standard electrode potential (-2.71 V vs standard hydrogen electrode) of sodium compared to Li (6.9 g mol^{-1} , -3.04 V vs standard hydrogen electrode), SIBs inevitably exhibit inferior energy density compared to LIBs. Consequently, to enhance the broader applicability and fully realize the potential of SIBs, one of the most efficient ways is to improve the operating voltages of the cathode to achieve higher

specific capacity, ultimately leading to the enhancement of energy density.[3]

State-of-the-art cathodes for SIBs can be mainly categorized into four types: 1) transition metal oxides, [4] 2) polyanionic compounds, [5] 3) Prussian blue analogs, [6] and 4) organic electrodes.^[7] In **Figure 1a**, we summarize the charge/discharge cut-off voltage and the specific capacity of representative SIB cathode materials. Among these cathodes, transition metal oxides and polyanion-type cathodes which possess high operating voltage and decent specific capacities, are considered the main options for constructing SIBs with higher energy and power density. Transition metal oxides of SIBs can be represented as Na, TMO₂ $(0 < x \le 1, TM = 3d \text{ element, e.g., Fe, Ni, Co, and Mn, etc.}),$ among which O3 and P2 phase oxides are two of the most investigated structures. Na_xTMO₂ layered oxides show the advantages of low cost, high theoretical capacity, and appreciable operating potential.^[8] Specifically, O3-type oxides possess higher capacity than the P2-type owing to the higher Na content while the complex phase transitions result in unsatisfactory cycling properties. P2-type oxides show a more stable structure over a wide voltage range, thus exhibiting improved capacity retention. [9] Polyaniontype electrode materials generally consist of MO_v [M represents a transition metal] polyhedral and $(XO_4)_m^{n-}$ or $(X_mO_{3m+1})^{n-}[X = S,$ P, Si, etc.] anion groups, which are connected by a corner and/or edge-sharing manner. Benefiting from the strong covalent

16146849, 2025, 15, Dwnholaded from https://advanced.onlinelibrary.wiely.com/oi/0101002/aem.2002405301 by University Town Of Shenzhen, Wiley Online Library on [17]11025]. See the Terms and Conditions (https://onlinelibrary.wiely.com/terms-and-conditions) on Wiley Online Library for rules of use; OA articles are governed by the applicable Centwice Commons

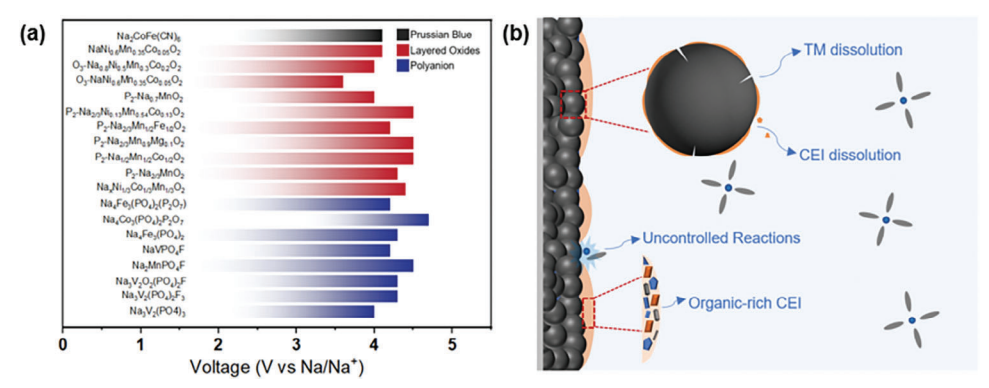


Figure 1. a) Work voltage comparison of various SIB cathodes in a half-cell (vs Na/Na⁺). b) The main challenges at the interface of high-voltage cathodes in sodium-ion batteries.

bonding of oxygen atom in the polyanion polyhedron, polyanion framework shows excellent structural stability. Some polyaniontype electrode materials with the formula of A_vMM'(XO₄)₃ such as Na₃V₂(PO₄)₃ (NVP) was classified as Na super-ionic conductor, which show favorable rate capacity by providing facile Na+ conducting channels in its crystal structure. The redox potential of the polyanion-type electrode can be tailored by combining polyanions with different degrees of inductive effect. For example, introducing anions with high electronegativity such as Fand $(P_2O_7)_4$ can effectively improve the working voltage of the cathode. By introducing F⁻ to NVP, the resultant Na₃V₂(PO₄)₂F₃ (NVPF) has attracted much attention for its high potential twostep redox plateaus of 3.7 and 4.2 V (vs Na+/Na), the high theoretical capacity of 128 mAh g⁻¹. Besides, although Prussian blue cathodes operate at lower voltages, their interfacial design strategies are still informative for high-voltage SIBs. Therefore, a few Prussian blue cathode interfacial design approaches are also included in this review.

However, higher operating voltages also present challenges to the interfacial stability of electrode and electrolyte, leading to the capacity decay over prolonged cycling. Regarding the bulk aspects of electrode, irreversible structural changes such as phase transitions and crystal lattice distortions often occur under highvoltage conditions. Additionally, higher cut-off voltages thermodynamically drive adverse reactions at interface, which are particularly notable due to their complexity and decisive role in battery performance.[10] The cathode interfacial evolution in SIBs mainly includes chemical/electrochemical reactions at the interface, as well as the consequent formation and evolution of interphases. Specifically, interfacial problems at high voltage can be mainly divided into the following points: 1) Electrolyte decomposition becomes significant at high voltages, particularly above 4.2 V, where electrolyte molecules undergo oxidation at the cathode interface, forming a thick and uneven interphase film. This increases interfacial resistance and deteriorates battery performance. Moreover, the parasitic oxidation of F-containing components, such as fluoroethylene carbonate (FEC) and NaPF₆, produces reactive HF or PF₅, which hydrolyze to form hydrofluoric acid (HF). The HF continuously erodes the cathode-electrolyte interphase (CEI), damaging the interface and accelerating transition metal dissolution. This issue is especially pronounced in layered oxides due to the catalytic activity of transition metals.[11] 2) Transition metal dissolution: Some layered oxide cathodes exhibit structural instability at high potentials, where transition metal ions within the lattice undergo valence state changes and dissolve into the electrolyte. Polyanion-type cathodes, such as NVPF, also experience transition metal dissolution at elevated voltages. As reported by Mariyappan and Tarascon, V dissolution increases with higher oxidation potential or state of charge in the NVPF electrode.[12] The dissolved metal ions may migrate to the anode, further damaging the solid-electrolyte Interphase (SEI) layer. 3) Poor stability of interphases: compared to LIBs, the electrolyte-electrode interphase (EEI) of SIBs exhibits higher fragility and solubility in electrolytes due to the milder acidity of Na+ compared to Li+, especially in the high potential range, that organic solvents decompose more intensely, leading to more unstable interphases. The dissolution of the CEI film leads to the re-exposure of the electrode surface to harmful interfacial reactions. Additionally, dissolved products of the SEI film on the anode can shuttle to the cathode, driven by concentration gradients, causing further degradation of the cathode.[13] (Figure 1b)

To construct robust and stable interphases and suppress harmful interfacial reactions, it is crucial to develop advanced characterization techniques to understand the formation and evolution mechanisms of interphases, while also designing tailored solutions to address interfacial challenges. Although some reviews have focused on the electrolyte-electrode interface of SIBs, a detailed summary specializing on the failure mechanism of CEI under high cut-off voltage, along with the corresponding optimization of electrolytes and electrode interphases, remains scarce. These two aspects are pivotal for high-energy-density SIBs and warrant further discussion. In light of the challenges faced by SIBs employing high-voltage cathodes, we discuss the emerging characterization techniques as well as the latest design strategies for electrolytes and cathode interfaces, aiming to offer an integrated design framework for high-energy-density SIBs. Finally, a prospect has also been made for the development and future application of SIBs.

2. Diagnostic Techniques for the Interface of SIB Cathode

The concept of the SEI was first introduced by Peled and colleagues in 1979, sparking extensive research into its chemical

16146840, 2025, 15, Downloaded from https://advancec

.com/doi/10.1002/aenm.202405301 by University Town Of Shenzhen, Wiley Online Library on [17/11/2025]. See the Terms

ditions) on Wiley Online Library for rules of use; OA articles are governed by the applicable Creative Commons

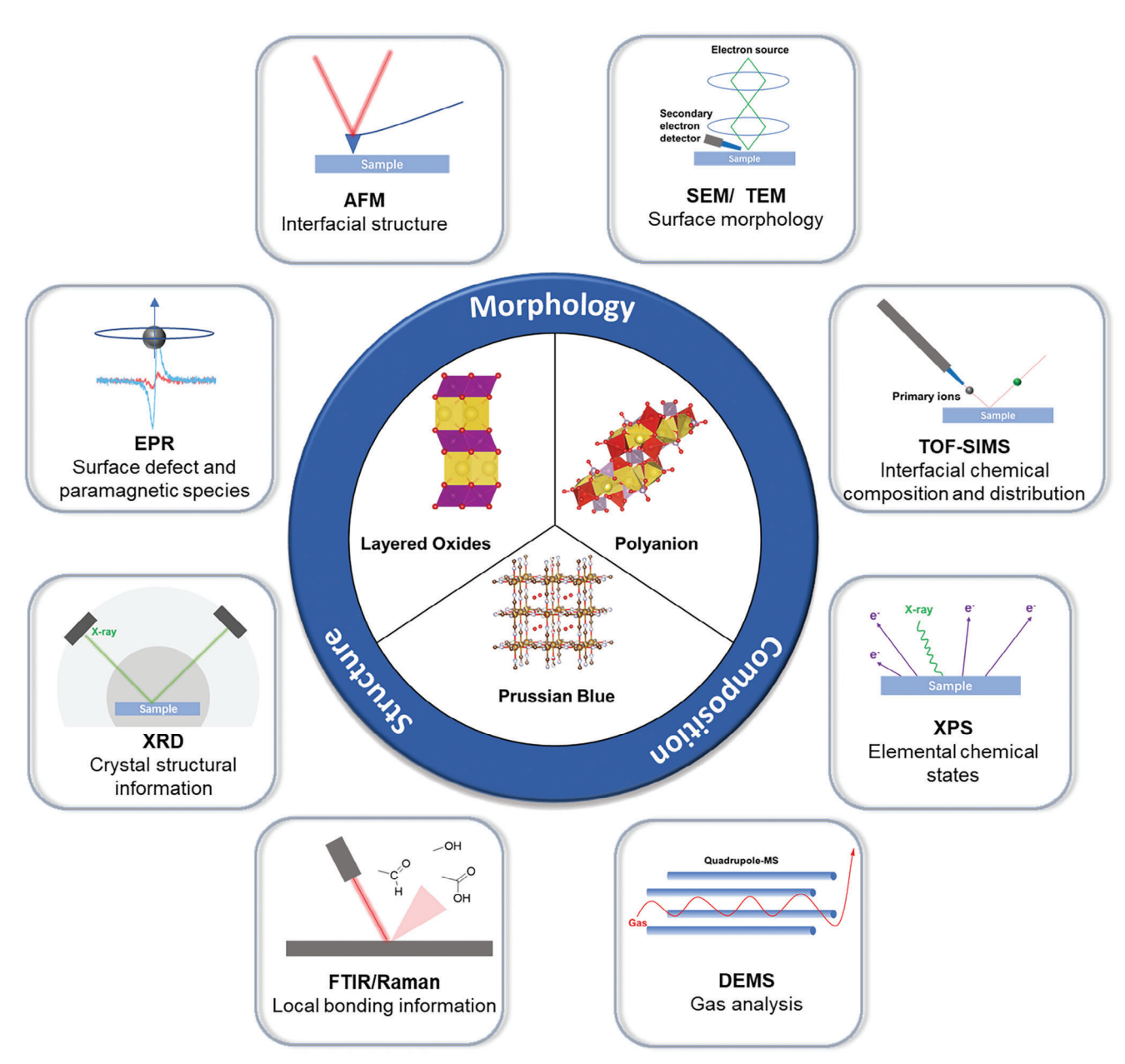


Figure 2. Characterization techniques commonly used for cathode interfaces (Outer); crystal structure diagrams of polyanionic cathode materials, Prussian blue, and layered oxide cathode materials in SIBs (Inner).

composition using a variety of analytical techniques.^[14] In contrast, the CEI is a relatively recent topic in battery research, gaining significant attention since the early 2000s. The conventional characterization techniques employed in SEI/CEI studies are summarized in Figure 2. Among them, scanning electron microscope (SEM), transmission electron microscope (TEM), and atomic force microscope (AFM) are essential tools for directly characterizing the surface features of sodium-ion battery cathodes.^[15] SEM provides detailed surface morphology and topography, TEM reveals internal structures and crystallography, and AFM measures surface roughness and mechanical properties. They offer a comprehensive view of both surface and internal characteristics, as well as mechanical behavior. In addi-

tion, spectral techniques provide unique insights into the cathode material's surface chemistry and electrochemical processes. Time-of-flight secondary ion mass spectrometry (TOF-SIMS), X-ray photoelectron spectroscopy (XPS), and Fourier transform infrared spectroscopy (FTIR) are valuable for analyzing the chemical composition of interfaces. Differential electrochemical mass spectrometry (DEMS) can be applied to analyze the gas components as the evolution of the interface. The combined use of multiple characterization techniques has become increasingly common in interface research. For instance, Wang et al.^[16] utilized TOF-SIMS, TEM, and SEM to demonstrate the distinct impact of weakly solvating solvents on interfaces. Their study revealed that the proportion of atomic fragments such as -CO₃

1614849, 2025, 15, Dwnholoded from https://a/wnneed.on/inlibitrary.wiely.com/oi/010.002/aem.20.02405301 by University Town Of Shenzhen, Wiley Online Library on [17]11025]. Se the Terms and Conditions (https://onlinelibitrary.wiley.com/terms-and-conditions) on Wiley Online Library for rules of use; OA articles are governed by the applicable Centwive Commons

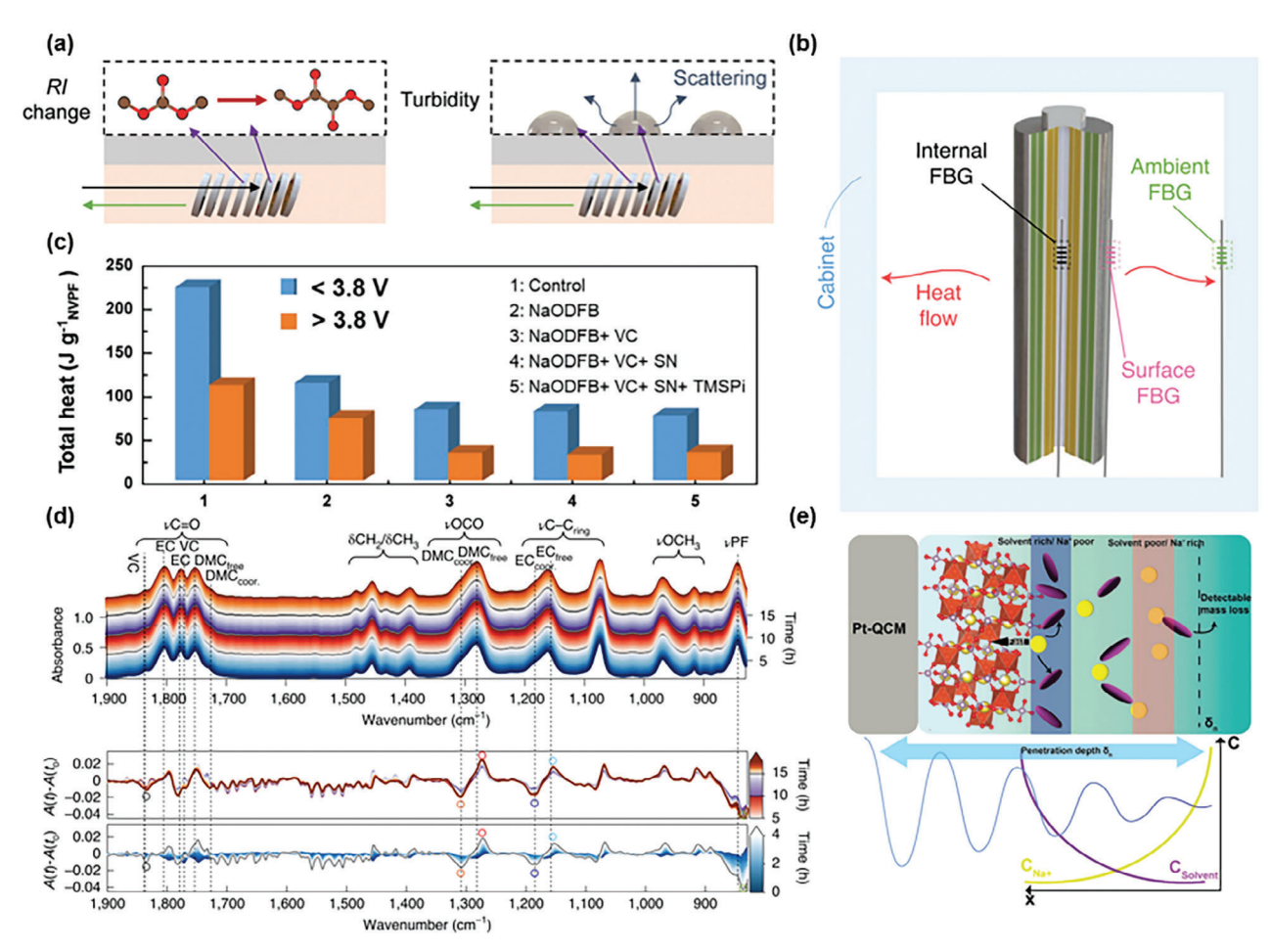


Figure 3. a) The phenomena of RI change arising from the (electro-)chemical reactions and the turbidity (g), respectively. Reproduced with permission. ^[19] copyright 2021, Royal Society of Chemistry. b) A schematic showing the set-up of optical sensing calorimetry. Reproduced with permission. ^[20] copyright 2020, Springer Nature. c) The total heat observed at < 3.8 V and >3.8 V as a function of electrolyte formulation. Reproduced with permission. ^[22] copyright 2021, Wiley-VCH. d) Absorbance spectra in function of the first charge (blue), first discharge (red), second charge (purple), and second discharge (orange). Reproduced with permission. ^[23] copyright 2022, Springer Nature. e) The model of opposing concentration gradient accentuated by the fast intercalation kinetics of the host NVP framework during reduction. Reproduced with permission. ^[24] copyright 2023, Wiley-VCH.

and $-C_x H_y O_z$ in the low-concentration (0.3 M) electrolyte (NVPF-W) is higher than in the 1.0 M electrolyte (NVPF-N), suggesting the formation of a denser CEI layer in the former. TEM images further confirmed that the CEI layer on the NVPF cathode in NVPF-W is more uniform and thinner (\approx 2 nm) compared to the rougher and thicker layer (2–8 nm) observed in NVPF-N.

Accurately and non-destructively characterizing interfaces has long been challenging due to their intrinsic inaccessibility and complex geometry. As high-voltage cathodes are developed, interface reactions become increasingly complex and hybrid. In this context, traditional characterization methods and time-consuming trial-and-error approaches are insufficient for identifying the chemical reactions or structural evolution occurring at the interface. Therefore, advanced techniques such as operando diagnostics^[17] and computational modeling^[18] are essential for probing interfacial dynamics and providing guidelines for electrolyte design and optimization. For instance, Tarascon et al.^[19] have developed various non-destructive characterization meth-

ods using optical sensors to gain a deeper understanding of battery interfaces. For example, the optical fiber Bragg grating (FBG) sensor can be utilized as a powerful tool to detect interfacial reactions in the dynamics of solvation. As shown in Figure 3a, electrolyte characteristics can be unraveled by monitoring refractive index (RI) change arising from the (electro-)chemical reactions and the turbidity. Compared with operando techniques such as TEM and NMR that inspect at the microscopic scale, optical sensors are more feasible to transplant to commercial batteries non-destructively. (Figure 3b) Besides, the FBG sensor provides critical parameters such as temperature (T), pressure (P), and strain (ϵ), which are linked to various interfacial reactions, including the formation and decomposition of the SEI/CEI. [20,21] By tracking the thermal events associated with these reactions, FBG can indirectly reflect the reactivity of electrolyte additives at the electrode-electrolyte interface, guiding the design of new electrolyte formulations.[22] (Figure 3c) When combined with spectroscopic techniques like infrared (IR) spectroscopy, the developed IR fiber evanescent wave spectroscopy (IR-FEWS) enables

ADVANCED ENERGY MATERIALS 16146840, 2025, 15, Downloaded from https://advanced.onlinelibrary.wiley.com/doi/10.1002/aemn.20240591 by University Town Of Shenzhen, Wiley Online Library on [17/11/2025]. See the Terms and Conditions (https://onlinelibrary.wiley.com/terms-

and-conditions) on Wiley Online Library for rules of use; OA articles are governed by the applicable Creative Commons

molecular identification and real-time monitoring of SEI/CEI formation processes.^[23] (Figure 3d) These devices offer a scalable solution for in-operando detection of electrode-electrolyte interphases. By integrating operando IR-FEWS, electrochemical quartz crystal microbalance (EQCM), and molecular dynamics simulations, researchers have meticulously characterized the differences between the interfaces of NVP and NVPF.[24] In the case of NVP, the high Na+ mobility in the bulk phase creates a reverse concentration gradient for uncoordinated solvent molecules, causing them to diffuse back into the electrolyte bulk, which the EQCM resonator detects as a mass loss. In contrast, with NVPF, the uncoordinated solvent molecules remain closer to the interface and do not diffuse as far away. (Figure 3e) Based on these insights, tailored strategies should be employed to address the specific challenges of different electrolyte/electrode interfaces. For instance, "soft-solvating" electrolytes can effectively facilitate the desolvation process in NVP, while a robust CEI is crucial for NVPF to prevent vanadium dissolution at high voltages, which can be achieved using localized high-concentration electrolytes (LHCE).

Advanced characterization methods can also be applied to investigate the degradation mechanisms of high-voltage cathode materials, such as oxygen-redox-active (ORA) layered oxides. ORA materials, which involve the redox of both transition metal cations and oxygen anions, offer enhanced average operating voltage and ultrahigh capacity. However, they suffer from significant voltage decay, the causes of which remain a topic of debate. Chen et al.[25] utilized a range of advanced analytical techniques and theoretical modeling, including in situ differential electrochemical mass spectrometry (DEMS), synchrotron-based hard and soft X-ray absorption spectroscopy (XAS), electron energy loss spectroscopy (EELS), and density functional theory (DFT) calculations, to uncover the degradation mechanism of the Oredox Na_{0.8}Li_{0.24}Al_{0.03}Mn_{0.73}O₂. Their findings indicate that oxygen escape typically results in the formation of oxygen vacancies, which propagate from the surface to the bulk of the material. These oxygen vacancies, in turn, generate a substantial number of structural defects during cycling, leading to phase boundaries and cracks within the cathode particles.

Future research is likely to prioritize the development of more sensitive in situ detectors and the integration of these techniques with advanced computational methods to more precisely simulate and predict interfacial reactions. Additionally, the effective application of these advanced characterization methods to practical battery systems, with the aim of enhancing overall performance and stability, will be a key area of focus. In summary, in situ characterization techniques are poised to play a pivotal role in advancing battery technology and in the creation of efficient, long-lasting energy storage solutions.

3. Dynamic Interplay Between the CEI and the Electrolyte

The relationship between the CEI and the electrolyte is crucial for battery performance and stability. The CEI forms at the cathode-electrolyte interface during chemical and electrochemical reactions, particularly at high voltages. A well-structured CEI facilitates Na⁺ transport while preventing harmful species from re-

acting with the cathode, maintaining efficient ion transport, and minimizing impedance. However, its composition and stability are strongly influenced by electrolyte components. In typical carbonate electrolytes, the CEI contains organic compounds from solvent oxidation (e.g., ethylene carbonate) and inorganic species like NaF from NaPF₆ decomposition. The introduction of fluorinated components, such as FEC, can increase the NaF content in the CEI, thereby enhancing its stability and improving ionic conductivity. However, unstable fluorine-containing species may decompose further, producing reactive by-products like HF and PF5. These by-products can exacerbate the dissolution of transition metals (e.g., Mn, Co, Ni), increasing resistance and ultimately leading to capacity decay. Over the course of cycling, especially at high voltages or elevated temperatures, the CEI can continuously evolve, reform, and even degrade, leading to fluctuations in impedance and performance. The ideal cathode-electrolyte interface (CEI) must exhibit excellent chemical and electrochemical stability across the battery's operating voltage range, preventing harmful side reactions. It should offer high ionic conductivity while maintaining electronic insulation to reduce charge transfer resistance and improve rate performance. The CEI must be mechanically robust, adapting to the volume changes of cathodes during cycling to maintain structural integrity. Additionally, it should adhere strongly to the cathode, be self-healing, and form through a controlled, reproducible process, ensuring long-term battery efficiency, safety, and lifespan. To regulate the formation of a high-performance CEI layer, one can tailor the electrolyte composition, such as using highly stable solvents or salts, which can mitigate harmful side reactions that degrade the CEI. Besides, certain additives can promote the creation of beneficial compounds in the CEI, such as NaF, which improve the protective properties of the layer. Another approach is to construct a protective layer ex situ on the cathode interface. For example, applying coatings to the cathode surface can help reduce direct contact between the cathode and the electrolyte, limiting electrolyte oxidation and CEI growth.

4. Solvent Molecule Manipulation

4.1. Carbonate

The development of ester-based solvents for lithium batteries began in the 1990s and led to the commercialization of propylene carbonate (PC)-based electrolytes in LIBs with LiCoO2 cathodes. Ongoing research continues to focus on improving stability, safety, and efficiency for high-performance applications.^[26] The electrolytes for SIBs have been developed based on those used in LIBs, utilizing the same anions and solvents. Consequently, ester-based solvents remain the most commonly used in SIB electrolytes. Despite extensive research aimed at optimizing electrolyte components to enhance various performance aspects, a universal electrolyte that meets all requirements has yet to be established. In 2012, Palacín et al. conducted a comparative study on a range of electrolyte formulations with different sodium salts and solvents. They found that the electrochemical performance of the electrolyte was highly dependent on the solvent used, with ethylene carbonate (EC) combined with PC emerging as the optimal formulation for enhancing the

16146484, 2025, 15, Dwnholaded from https://dwnneed.onlinelibrary.wiely.com/oi/01002/aen.20.2945301 by University Town Of Sheraben, Wiley Online Library on [17/11/1225]. See he Terms and Conditions (https://onlinelibrary.wiely.com/terms-and-conditions) on Wiley Online Library for rules of use; OA articles are governed by the applicable Cerative Commons

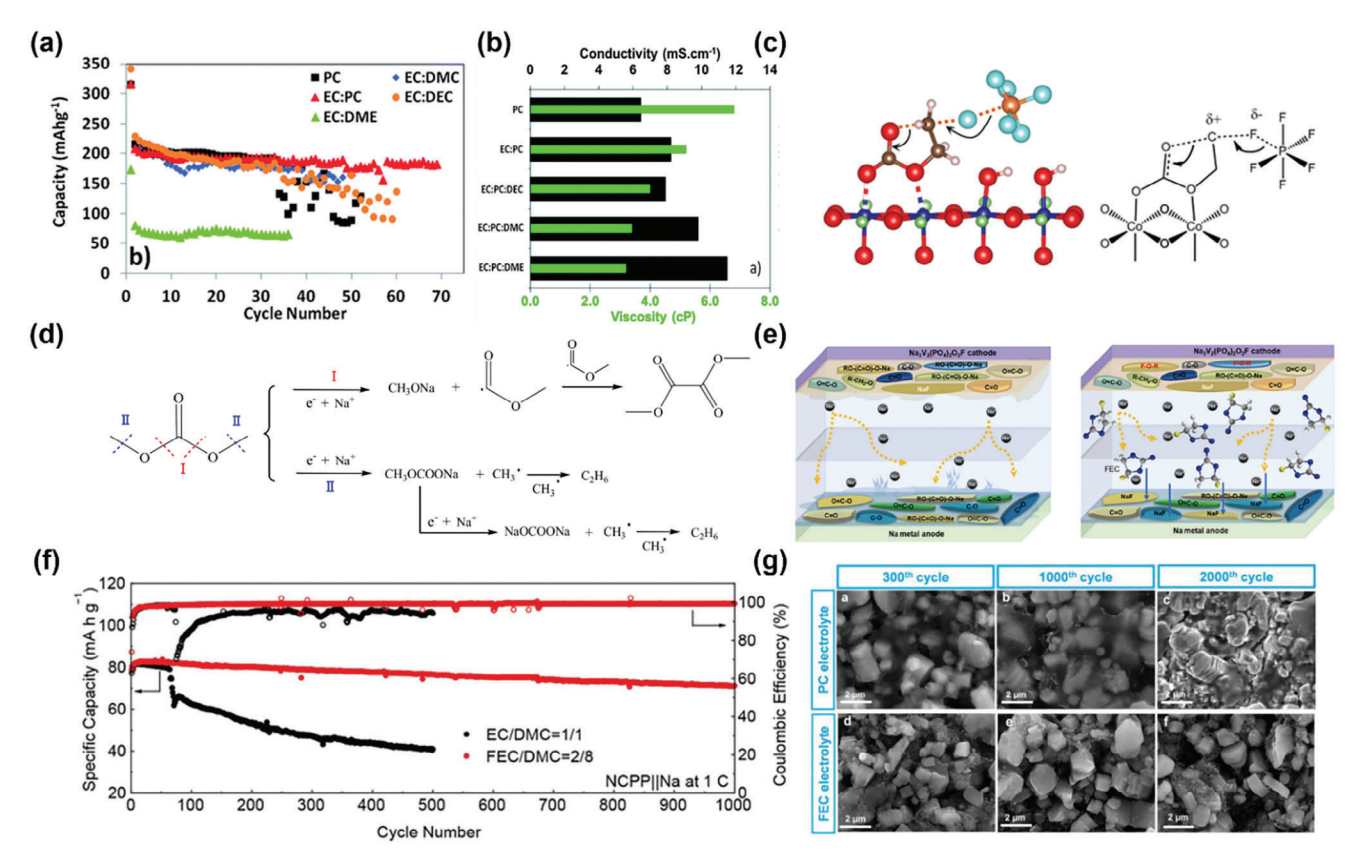


Figure 4. a) Discharge capacity versus cycle number for the corresponding cells with different electrolytes. Reproduced with permission. [27] copyright 2012, Royal Society of Chemistry. b) Conductivity (black bars and upper x axis) and viscosity (green bars and lower x axis) values of electrolytes based on 1 M NaClO₄ dissolved in various solvent mixtures. Reproduced with permission. [29] copyright 2013, Royal Society of Chemistry. c) Ring-opening reaction of an adsorbed EC activated by the LiCoO₂ surface acting as a Lewis acid. Reproduced with permission. [31] copyright 2016, American Chemical Society. d) The reduction pathway of DMC at the HC electrode. Reproduced with permission. [37] copyright 2018, IOP Publishing. e) The EEI schematic diagrams of unfluorinated treatment (left) and fluorinated treatment (right). Reproduced with permission. [38] copyright 2023, Wiley-VCH. f) Cycling performance of Na₄Co₃ (PO₄)₂P₂O₇/Na cells in EC/DMC = 1/1 and FEC/DMC = 2/8 based electrolyte at 1 C. Reproduced with permission. [40] copyright 2022, Wiley-VCH. g) SEM images of Na_{2/3} Ni_{1/3} Mn_{2/3}O₂ cathodes after 300, 1000, and 2000 cycles at 5 C in the PC electrolyte and FEC electrolyte. Reproduced with permission. [42] copyright 2021, Wiley-VCH.

performance of hard carbon (HC) anodes.[27] (Figure 4a) EC and PC are widely used in LIBs due to their ability to effectively dissociate lithium salts and form a protective film on both the cathode and anode. For instance, Choi reported that EC/PCbased electrolytes do not undergo electrochemical decomposition when the cathode is charged up to 4.2 V (vs Na/Na+), and the use of this electrolyte significantly enhances the electrochemical performance of the Na₄Fe₃(PO₄)₂(P₂O₇) cathode. [28] Besides, adding linear esters such as dimethyl carbonate (DMC) to the binary electrolyte system can further improve the performance of the electrolyte by reducing the viscosity and melting point of the electrolyte. (Figure 4b) For instance, EC_{0.45}:PC_{0.45}:DMC_{0.1} with 1 M of Na-salt was identified by Palacín et al. as optimal for Na-ion batteries. The solvation shell of sodium cations is mainly composed of EC, which is certainly also related to the observation of EC decomposition products being the main constituent of the CEI layer. [29] According to Johansson et al. sodium bis(trifluoromethylsulfonyl)imide (NaTFSI) and NaPF₆ in EC_{0.45}:PC_{0.45}:DMC_{0.10} exhibit similarities to conventional LIB electrolytes both in terms of physico-chemical and molecular properties.^[30] Although there are limited studies on SIBs, the instability of EC at cathode interfaces has been documented in LIB research.^[31–33] (Figure 4c) It is important to note that electrochemical stability limits are typically assessed using inert electrodes. However, in practical applications, the catalytic nature of the electrode surface can trigger solvent oxidation at lower voltages, potentially within the operating range of the cathode. As a result, electrolyte stability on active electrodes is often more influenced by kinetic factors and the presence of chemical passivation layers than by thermodynamics alone.^[27] In practice, ester-based electrolytes containing EC still fall short of meeting the requirements for high-voltage cathodes.

EC has long been regarded as an essential component of organic electrolytes. However, the concept of EC-free electrolytes has recently gained traction in the development of LIBs. [34] Avoiding the use of unstable EC while retaining linear carbonates offers a promising approach for advancing electrolytes suitable for high-voltage cathodes in both LIBs and SIBs. For instance, Ma et al. systematically investigated electrolytes using NaPF₆ as the solute and the mixture combined linear carbonates such as ethyl methyl carbonate (EMC), DMC, or diethyl carbonate (DEC) with cyclic carbonates such as PC or EC as the solvent. They concluded

16146484, 2025, 15, Dwnholaded from https://dwnneed.onlinelibrary.wiely.com/oi/01002/aen.20.2945301 by University Town Of Sheraben, Wiley Online Library on [17/11/1225]. See he Terms and Conditions (https://onlinelibrary.wiely.com/terms-and-conditions) on Wiley Online Library for rules of use; OA articles are governed by the applicable Cerative Commons

that PC-based electrolytes outperform EC-based ones in terms of capacity retention and safety. With the further introduction of multiple additives, the optimized electrolyte (0.8 M NaPF₆/PC-EMC) in a NaNi_{1/3}Fe_{1/3}Mn_{1/3}O₂/HC cell achieved 56.16% capacity retention at -40 °C and retained 80% capacity after more than 2500 cycles.[35] The PC/EMC electrolyte further enhances the formation of a protective interfacial layer, effectively mitigating parasitic reactions on the cathode surface and suppressing the chemical dissolution of transition metal ions from the NaNi_{1/3}Fe_{1/3}Mn_{1/3}O₂ electrode. [36] However, the reduction of linear esters at low voltages is a concern, particularly in SIBs with a sodium metal anode. Linear carbonates are less stable than cyclic carbonates at low potentials, leading to a shuttle mechanism where dissolved species from the reduction of linear carbonates on the carbon electrode migrate to the cathode and are oxidized. This process results in significant Na ion loss in the full cell.[37] (Figure 4d).

Compared to alkyl carbonates, fluorinated carbonates theoretically have lower highest occupied molecular orbital (HOMO) energy, making them more thermodynamically stable against oxidation. A typical example is FEC, which substitutes the methyl group in PC with a fluorine atom. Some studies have shown that FEC positively contributes to the formation of the CEI when used as a solvent, although the underlying mechanism remains unclear. Wu et al.[38] constructed a bidirectional fluorine-rich film on Na₃V₂(PO₄)₂O₂F using 1 M NaClO₄ as the salt and a mixture of FEC and PC (1:9 v/v) as the main solvents. The resulting Na₃V₂(PO₄)₂O₂F/carbon cloth full cells exhibited minimal capacity attenuation, as low as 0.01%, within a voltage range of 2-4.3 V. Further analysis revealed that FEC not only suppresses the continuous decomposition of solvated PC but also promotes the formation of a fluorine-rich CEI at high potentials. Consequently, the resulting CEI, with a reduced thickness of 5.76 nm, exhibits enhanced Na+ transport capabilities. (Figure 4e) However, according to Sun et al.[39] the FEC additive and NaClO₄ salt may continuously decompose on the surface of the Na₃(VO_{1-x}PO₄)₂F_{1+2x} cathode, leading to the formation of an uneven CEI, which results in deteriorated cycle stability and increased transfer resistance. Given the ongoing controversy, further investigation into the reaction mechanism of FEC on Na₃(VO_{1-x}PO₄)₂F_{1+2x} is necessary. Chou's group[40] reported that a FEC-based electrolyte (1 M NaPF₆ in FEC/DMC = 2/8 by volume) is well-suited for Na₄Co₃(PO₄)₂P₂O₇, forming a NaF-rich CEI film that effectively prevents the cathode from reacting with the electrolyte. At a high cutoff voltage of 4.7 V, the Na₄Co₃(PO₄)₂P₂O₇/Na half-cell demonstrated a capacity retention of 89.99% after 1000 cycles at 1 C. (Figure 4f) The use of FEC as a solvent also extends to layered transition metal oxides. As early as 2015, Hassoun et al.[41] reported that adding FEC to a PC-based electrolyte significantly improved the cycling performance of Na_{0.6}Ni_{0.22}Fe_{0.11}Mn_{0.66}O₂/Sb-C full cells. Following this, Zhang et al. [42] utilized FEC as the sole solvent, achieving 94% capacity retention after 1000 cycles at 5 C in a Na_{2/3}Ni_{1/3}Mn_{2/3}O₂/HC full cell. Through DFT and ab initio molecular dynamics (AIMD) simulations, they attributed the exceptional electrochemical performance to FEC's higher oxidation stability compared to PC, which promotes the formation of a robust CEI and prevents continuous electrolyte consumption. (Figure 4g)

4.2. Ether

Electrolytes for SIBs can generally be categorized into carbonatebased and ether-based types. Carbonate solvents are typically the preferred choice for pairing with high-voltage cathodes (>4.2 V) due to their oxidation stability. However, carbonate solvents often show incompatibility with many anodes, particularly conversiontype and alloy materials. The significant volume changes of these anodes during cycling lead to excessive solvent decomposition and the formation of SEI layers with low mechanical strength, resulting in irreversible capacity fading. In contrast, ether-based electrolytes offer better compatibility with anodes, and their relatively low melting points and viscosity enable SIBs to operate over a wider temperature range. However, ether-based electrolytes suffer from an inherent lack of oxidation resistance. Therefore, extending the electrochemical stability window (ESW) of etherbased electrolytes through rational design strategies can provide an additional electrolyte option for high-voltage SIBs, allowing them to function under a broader range of operating conditions.

Recent studies have shown that ethers are compatible with various polyanionic cathodes in sodium batteries, and the synergy between ether solvents and salts is critical for both ESW and CEI formation. For example, it has been reported that a diglyme-based electrolyte with NaPF₆ as the salt enables stable cycling and fast charge-transfer in NVPF, with a cutoff voltage of up to 4.3 V. This stability may be attributed to the polymerinorganic CEI formed on the NVPF electrodes. [43,44] (Figure 5a) In addition to enhancing interfacial properties, diglyme also contributes to the bulk structural stability of NVPF.[45] Basak et al. prepared a series of electrolytes and compared their physicochemical and electrochemical properties before testing their performance with the Na₃(VOPO₄)₂F electrode. The linear sweep voltammetry (LSV) profiles obtained for all electrolyte compositions demonstrated anodic stability above 4.8 V against stainless steel electrodes, making them suitable for pairing with sodium vanadium fluorophosphate electrodes. (Figure 5c) The investigations revealed that diglyme acts as an effective stabilizing agent for the electrode-electrolyte interface when added to either EC/DEC or EC/PC. This study also identified two promising electrolyte compositions EC/DEC/diglyme (2:2:1) + 1.0 M NaClO₄ and EC/PC/diglyme (2:2:1) + 1.0 M NaClO₄ suitable for SIBs. [46] Furthermore, the oxidation stability of ether-based electrolytes can be enhanced by employing additive strategies or by achieving high Na+ coordination with minimal free solvents, which will be discussed in detail in sections 6, respectively. Another strategy to improve oxidation resistance is the introduction of multiple co-solvents. For example, You et al.[44] utilized tetrahydrofuran (THF) as the main solvent, combined with PC and ethoxy(pentafluoro)cyclotriphosphazene (PFPN) as co-solvents. The resulting electrolyte not only maintains the low-temperature advantages of the ether solvent but also demonstrates improved antioxidant capabilities, attributed to the formation of a P- and F-rich CEI on the cathode. (Figure 5b,d)

4.3. Sulfone

Sulfone-based electrolytes exhibit excellent oxidation stability, along with high boiling and flash points, despite their poor

16146840, 2025, 15, Downloaded from https://advanced.onlinelibrary.wiley.com/doi/10.1002/aenm.202405301 by University Town Of Shenzhen, Wiley Online Library on [17/1/12025]. See the Terms

and Conditions (https://onlinelibrary.wiley.com/terms

and-conditions) on Wiley Online Library for rules of use; OA articles are governed by the applicable Creative Commons

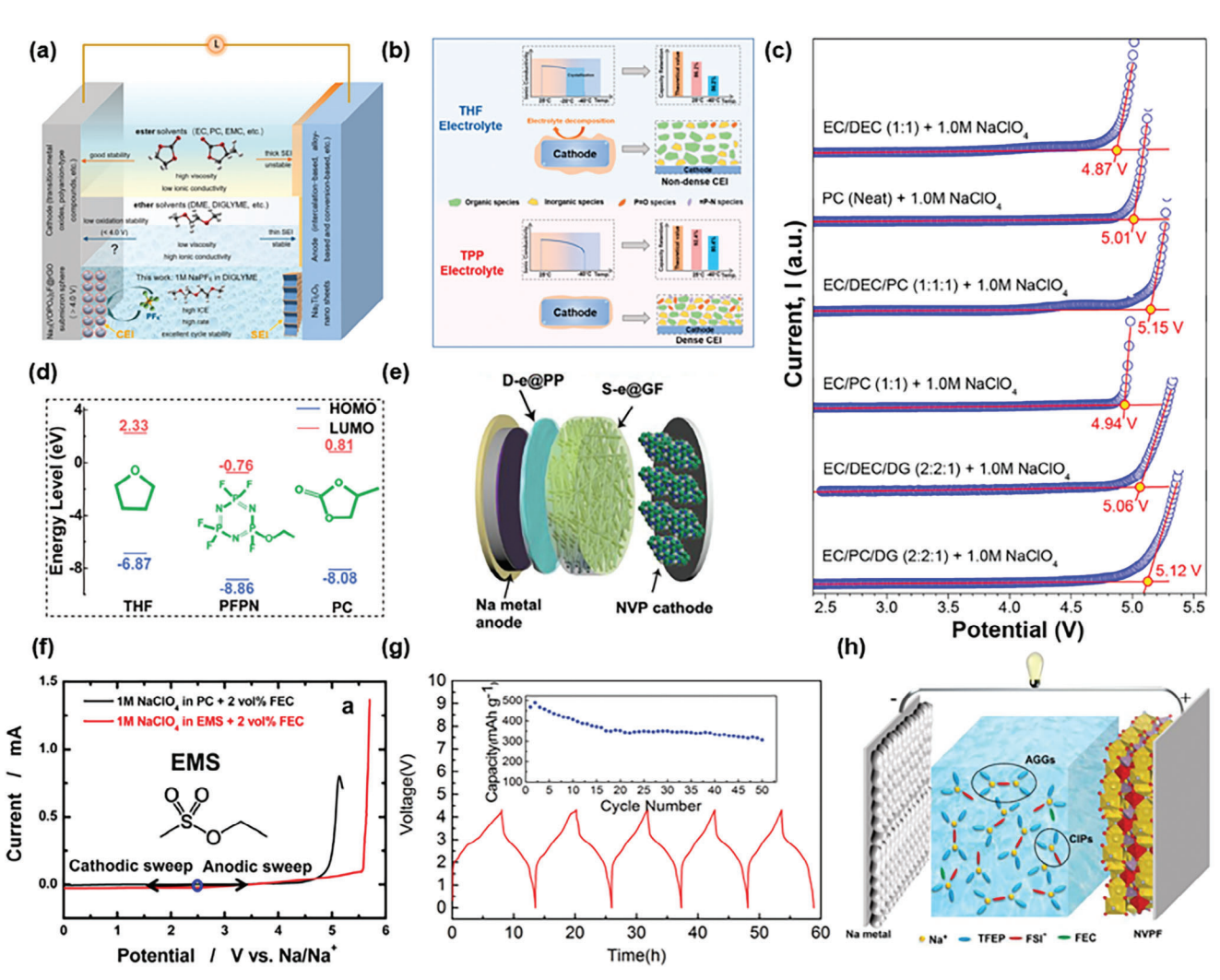


Figure 5. a) Illustration of effects of electrolyte system on full cell. Reproduced with permission. [43] copyright 2022, Elsevier. b) Schematic illustration of the working mechanism of selected electrolyte in the Na_{2/3} Mn_{2/3} Ni_{1/3} O₂ cathode. Reproduced with permission. [44] copyright 2023, American Chemical Society. c) Typical linear sweep voltammetry (LSV) plots obtained with various electrolyte compositions. Reproduced with permission. [46] copyright 2023, American Chemical Society. d) LUMO/HOMO energy level diagram including solvents. Reproduced with permission. [47] copyright 2023, American Chemical Society. e) Schematic of proposed full battery configuration. Reproduced with permission. [47] copyright 2022, Elsevier. f) Linear sweep voltammetry of a sodium cell using two electrolytes, namely, 1 M NaClO4 in PC + 2 vol % FEC and 1 M NaClO₄ in EMS + 2 vol % FEC. Reproduced with permission. [48] copyright 2014, American Chemical Society. g) Charge/discharge curves and cycling performance of Sb/NaNi_{0.35} Mn_{0.35} Fe_{0.3} O₂ cells in the 0.8 M NaPF₆/TMP + 10 vol% FEC electrolyte. Reproduced with permission. [57] copyright 2016, Wiley-VCH. h) Schematic illustration of SIBs with the TFEP-based electrolyte. Reproduced with permission. [57] copyright 2022, American Chemical Society.

reduction resistance and limited SEI-formation capability at the anode. Compared to carbonyl groups in carbonates and ether groups in oligoethers, the stronger electron-withdrawing sulfonyl group lowers the HOMO energy level, resulting in enhanced oxidation stability. Wu et al. [47] designed an innovative structure incorporating two types of electrolytes supported by a polypropylene separator and a glass fiber separator, respectively. (Figure 5e) The excellent oxidation stability of sulfone-based electrolytes supports the cycling of NVP, while the diglyme-based electrolyte on the anode side provides an ideal environment for Na metal. Sun et al. [48] applied a sulfone-based electrolyte in a unique battery system with a carbon-coated Fe $_3$ O $_4$ anode and a NaNi $_{0.25}$ Fe $_{0.5}$ Mn $_{0.25}$ O $_2$ layered cathode. The anodic stability of the electrolyte was further increased to 5.6 V versus Na/Na $^+$ by re-

placing PC with ethyl methyl sulfone, with 2 vol% FEC added as an additive to enhance the anode's stability. (Figure 5f)

4.4. Alkyl Phosphate

Alkyl phosphates are known for their favorable nonflammability and oxidation stability. [49] Cao et al. [50] reported a nonflammable phosphate-based electrolyte using trimethyl phosphate (TMP) as the solvent and 10 vol% FEC as an additive. This electrolyte exhibits a wide ESW (0–4.5 V vs Na/Na⁺) and demonstrates excellent compatibility with the NaNi $_{0.35}$ Mn $_{0.35}$ Fe $_{0.3}$ O $_2$ cathode. (Figure 5g) In addition to TMP, triethyl phosphate (TEP), which has a similar structure, is also used as a nonflammable solvent

16146840, 2025, 15, Downloaded from https://advanced.onlinelibrary.wiley.com/doi/10.1002/aemm.202405301 by University Town Of Shenzhen, Wiley Online Library on [17/11.2025]. See the Terms and Conditions (https://onlinelibrary.wiley.com/terms-and-conditions) on Wiley Online Library for rules of use; OA attacks are governed by the applicable Certain Commons

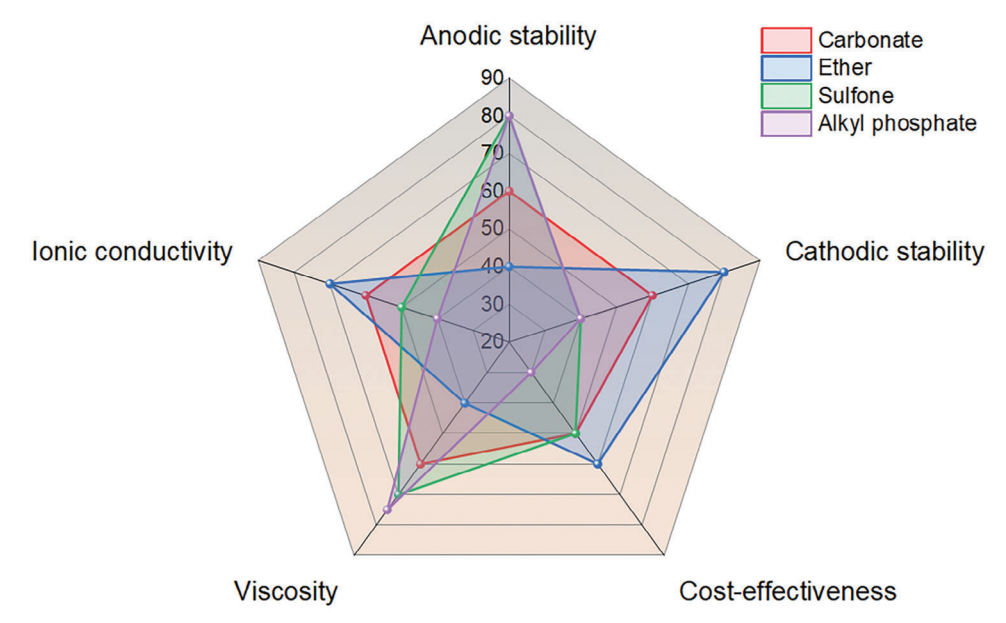


Figure 6. The performance comparison radar chart of different types of electrolyte solvents. [59]

and shows good compatibility with various polyanion cathodes, such as $Na_3V_2(PO_4)_3$, [51] $Na_3V_18Zn_02(PO_4)_3$, [52] and NVPF. [53] However, it is important to note that organophosphorus compounds like TMP and TEP have poor SEI-forming capabilities on anodes. Therefore, film-forming additives such as FEC, sodium bis(oxalate)borate (NaBOB), or vinylene carbonate (VC) are typically added to these phosphorus-based electrolytes.^[52,54] Another approach to addressing this issue is to reduce the amount of free solvent by using specific additives or by creating a highly concentrated electrolyte system. For instance, Pan et al.[55] used trifluorotoluene as a "solvent coordinator" to suppress free TEP molecules. The optimized electrolyte enabled a NaCu_{1/9}Ni_{2/9}Fe_{1/3}Mn_{1/3}O₂/HC full cell to cycle steadily for 400 cycles with high coulombic efficiency (>99.95%) at 0.2 C. Zhang et al.[56] developed a nonflammable phosphate electrolyte with sodium bis(fluorosulfonyl)imide (NaFSI) at an optimized molar ratio of 1:1.5, which effectively forms a stable electrodeelectrolyte interphase on both the cathode and anode. The dense and uniform CEI minimizes surface reconstruction on the cathode and prevents the dissolution of transition metals, achieving a capacity retention of 83.5% after 200 cycles at 0.2 C in a NaNi_{0.68}Mn_{0.22}Co_{0.10}O₂/HC full cell. However, the high cost and poor wettability hinder the broader application of such concentrated electrolyte systems. A more straightforward approach is to modify the structure of organophosphorus molecules through fluorination. By substituting the alkyl hydrogen in TEP with fluorine, tris(2,2,2-trifluoroethyl) phosphate (TFEP) is obtained, which has reduced polarity. The TFEP solvent exhibits incomplete coordination to Na⁺, allowing more anions to enter the solvation sheath of Na+, forming ionic aggregates (AGGs) and contact ion pairs (CIPs), resulting in an anion-induced ion-solventcoordinated structure. (Figure 5h)[57,58]

The development of high-voltage SIBs requires careful consideration of electrolyte solvents to ensure stability, high ionic conductivity, and compatibility with electrode materials as well as $sodium\ salts\ (such\ as\ NaPF_6\ or\ NaClO_4)$ at wide ESW. Com-

pared to LIBs, SIBs face unique challenges that necessitate differences in electrolyte design. Sodium ions have a larger ionic radius compared to lithium ions, which impacts their solvation and transport properties in the electrolyte. This larger size results in lower ionic mobility and higher activation barriers for sodiumion transport, which in turn affects the electrolyte's overall performance. To address these issues, the electrolytes used in SIBs often incorporate solvents with lower viscosity and higher ion mobility, such as PC and diglyme, as they can better accommodate the larger sodium ions. Other, organic carbonate solvents, such as EC, DEC, and FEC are widely employed due to their high dielectric constants and ability to dissolve sodium salts, thus ensuring sufficient ionic mobility. Beyond carbonates, several alternative solvents, such as ethers, phosphate esters, and sulfones, have been explored for high-voltage SIBs due to their unique properties. The consideration of solvents for industrialized sodium-ion batteries is multifaceted. Currently, the electrolyte solvents for sodium-ion batteries are still primarily based on carbonates due to their well-rounded performance. For batteries operating in specialized environments (such as extremely low temperatures, high temperatures, or high charge/discharge rates), suitable alternatives can be selected based on the performance characteristics of different solvents. (Figure 6).

5. Solute Anion Manipulation

The species and concentration of salts significantly affect the macroscopic physico-chemical properties of the electrolyte, such as ionic conductivity and viscosity, as well as the microstructure, including solvation and ion-pairing. Sodium salts currently investigated for use in SIB electrolytes each have specific advantages and limitations. (**Figure 7a**) For instance, NaClO₄ and NaPF₆ are the two most commonly used sodium salts in SIBs. Recent studies have shown that NaPF₆-based electrolytes facilitate the formation of a dense and robust cathode–electrolyte interphase (CEI) on layered oxides, effectively preventing the

16146484, 2025, 15, Dwnholaded from https://dwnneed.onlinelibrary.wiely.com/oi/01002/aen.20.2945301 by University Town Of Sheraben, Wiley Online Library on [17/11/1225]. See he Terms and Conditions (https://onlinelibrary.wiely.com/terms-and-conditions) on Wiley Online Library for rules of use; OA articles are governed by the applicable Cerative Commons

www.advancedsciencenews.com

www.advenergymat.de

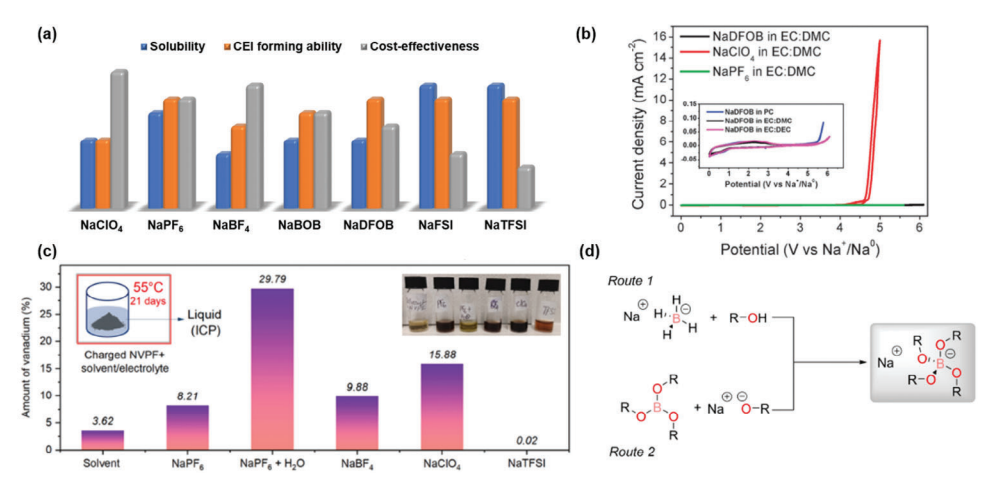


Figure 7. a) Comparison of performance indicators of common sodium salts including solubility, CEI forming ability, and cost-effectiveness. [67] b) CVs of the cells with electrolytes of 1.0 M NaX (X = DFOB, ClO₄, and PF₆) in EC: DMC. Reproduced with permission. [61] copyright 2015, Royal Society of Chemistry. c) Amount of vanadium dissolved from the charged NaV₂(PO₄)₂F₃ powder leached in EC-PC-DMC without or with different Na-salts at 55 °C for 21 days. Reproduced with permission. [12] copyright 2023, Elsevier. d) The synthetic routes to prepare a wide range of borate anions. Reproduced with permission. [64] copyright 2022, Wiley-VCH.

dissolution of transition metal ions. In contrast, the CEI formed in NaClO₄ electrolytes contains more organic and fewer inorganic components, which negatively impacts rate capability and cycling stability.^[60] However, the hydrolysis of NaPF₆ generates aggressive HF, which tends to corrode the CEI and react with carbonate molecules. Other salts, such as sodium tetrafluoroborate (NaBF₄), NaFSI, and NaBOB, have also been explored as candidates for SIB electrolytes. Among these, NaBF₄-based electrolytes face challenges due to their moderate dissociation constant and conductivity. NaTFSI or NaFSI-based electrolytes demonstrate a lower tendency for HF formation and exhibit nearly negligible vanadium dissolution from NVPF.[12] (Figure 7c) However, NaFSI suffers from a limited ESW, and aluminum corrosion in NaFSI-based electrolytes hinders its broader application. Therefore, developing new sodium salts for electrolytes or the synergistic use of multiple salts is crucial for enhancing the overall performance of SIB electrolytes.

Boron-based anions have garnered significant research interest in LIBs, leading to the development of salts such as Lithium Bis(oxalate)Borate (LiBOB) and lithium difluoro(oxalate)borate (LiDFOB). Inspired by these advancements, sodium analogs have been adapted for use in SIB electrolytes. For instance, sodium difluoro(oxalato)borate (NaDFOB) demonstrates enhanced solubility and an ESW comparable to that of NaPF₆ in carbonate electrolytes. (Figure 7b) Moreover, NaDFOB exhibits superior ion conductivity, rate capabilities, and cycling performance compared to NaClO₄ and NaPF₆^[61] Its robust nature makes it an ideal choice for maintaining stable electrolyte-electrode interfaces, even under high-voltage conditions.^[62,63] Wright et al.^[64] designed and synthesized a series of sodium borate salts for use as electrolyte components. (Figure 7d) Commercial pouch cells cycled with the optimized sodium salts Na[B(hfip)4] DME (1a) and Na[B(pp)₂] (1b') demonstrated enhanced cycling stability compared to the conventional NaPF₆ salt. Additionally, the [B(pp)₂] anion exhibits a high tolerance to air and moisture. Shanmukaraj et al.^[65] introduced Na₂C₃O₅ as a highly efficient, cost-effective, and safe cathode sodiation additive. The $Na_2C_3O_5$ additive improves the surface morphology of $P2-Na_{2/3}Mn_{0.8}Fe_{0.1}Ti_{0.1}O_2$ while maintaining the chemical composition of the CEI film. Moreover, high operating voltages and good rate capabilities in SIBs can be achieved by combining anion intercalation with a multi-ion design strategy. For example, introducing LiPF $_6$ into a NaPF $_6$ -based carbonate electrolyte at a ratio of 30 at% significantly improves the diffusion kinetics of SIBs. The resulting full cells exhibit a high mid-operating voltage of \approx 4.0 V and deliver a rate capability of up to 30 C.[66]

An ideal sodium salt should possess excellent solubility, high chemical and electrochemical stability, and the ability to interact synergistically with the solvent to form a robust CEI. Common choices, such as NaPF $_6$, are favored for their high solubility in organic solvents and ability to form stable SEI layers on the anode. However, above 4.3 V, NaPF $_6$ tends to decompose, producing harmful byproducts such as HF, which can induce side reactions with both the electrolyte and electrode materials. This issue can be addressed through the synergistic use of multiple sodium salts or by incorporating electrolyte additives. For example, the combination of NaPF $_6$ with NaTFSI or NaBF $_4$ can simultaneously improve conductivity, stability, and battery cycle life. Such dual-salt or multi-salt systems can offer a broader ESW and enhance the quality of the passivation layer at the electrode interface.

6. Regulation of Solvent-Ion Interactions

6.1. High-Concentration Electrolytes

The aforementioned strategies primarily optimize electrolytes by altering solvent species, and changing salts, all of which have been proven effective in modifying the physicochemical properties of the electrolyte and constructing a better CEI for high-voltage cathodes. Recently, many studies have focused on regulating the solvation environment of Na⁺, which has been shown to be crucial for the cyclability of high-voltage cathodes. Similar to LIBs, the solvation structure in SIBs can be roughly classified into three types: 1) solvent-separated ion pairs (SSIPs), 2) CIPs, and

16146840, 2025, 15, Downloaded from https://advance.

.com/doi/10.1002/aenn.202405301 by University Town Of Shenzhen, Wiley Online Library on [17/11/2025]. See the Terms and Conditions (https://onlinelibrary.wiley.com/terms

and-conditions) on Wiley Online Library for rules of use; OA articles are governed by the applicable Creative Commons

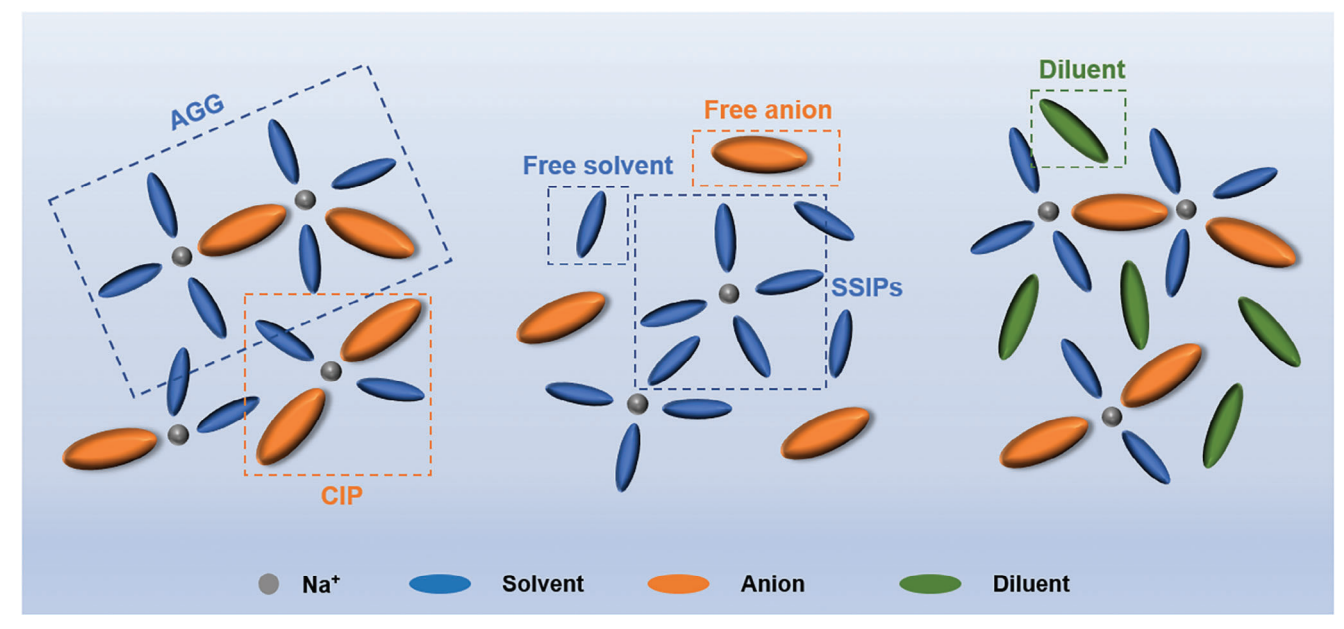


Figure 8. Three typical solvation environments in SIB electrolytes.

3) AGGs. The composition and structure of these solvation complexes can significantly impact the formation and evolution of the EEI, which is closely related to the battery's cycle life, rate capacity, energy density, and safety. For example, by increasing the salt concentration to above 3 M, high-concentration electrolyte (HCEs) enable nearly all solvent molecules and anions to coordinate with lithium ions. The reduction of free solvent molecules in the solvation structure leads to a wider operating voltage window and promotes the formation of a stable inorganic-rich CEI constructed by anions. However, HCEs face challenges such as highcost and high-viscosity, which hinder their commercialization. Inert diluents, such as perfluoroether, are miscible with the highconcentration electrolyte but do not participate in lithium ion coordination, thereby preserving the unique solution structure of the HCEs in the localized environment, which is commonly referred to as localized high-concentration electrolyte (LHCEs). LHCEs not only reduce the lithium salt content in the electrolyte, effectively lowering both the viscosity and cost, but also maintain excellent electrochemical performance due to the enhanced interfacial stability. Using HCEs or LHCEs has been shown to be effective in both LIBs and SIBs, as these methods facilitate the formation of AGGs and CIPs in the electrolyte, leading to the development of anion-dominated CEI or SEI. (Figure 8) According to Xu et al., the solvation trends of Na⁺ are similar to those of Li⁺ in carbonate electrolytes; however, the ion-solvent distances for Na+ are longer than for Li+, and Na+ has a greater tendency to form contact pairs in linear carbonate solvents (Figure 9a). Compared to Li⁺, the larger size of Na⁺ and its weaker interactions with solvents provide more opportunities for anions to participate in the solvation shell.^[68] Furthermore, NaPF₆ exhibits higher ionic conductivity, cation transference number, and binary diffusion coefficient compared to LiPF₆, leading to superior performance at high C-rates. [69] (Figure 9b)

Conventional electrolytic systems with moderate salt concentrations (0.8–1.5 M) suffer from the decomposition of free solvent

molecules on the cathode surfaces which leads to the formation of unstable CEI. HCEs with a salt concentration of up to 3 M produces salt-solvent complexes including CIPs and AGGs which allow the formation of inorganic-dominated CEI thus stabilizing the cathode. In the past few years, increasing salt concentration has proved to be an effective strategy for lithium batteries due to its capability to construct an effective EEI which is also applicable for SIBs. For example, Choi et al.[70] construct an ultraconcentrated NaFSI-based electrolyte for high-voltage cathodes that exhibit over 4.9 V versus Na/Na+. Such oxidation durable electrolyte enables outstanding cycling stability of Na/Na₄Fe₃(PO₄)₂(P₂O₇) cells. (Figure 9c) However, the expensive high-concentration electrolyte may make the SIBs lose the advantage of low cost and difficult to use in practice. One way to reduce costs and retain the characteristics of high concentration electrolytes is to use diluents. For example, Qiu et al.[71] produce an enhanced anionderived and inorganic components-dominated solid electrolyte interphases by introducing a low permittivity (4.33) bis(2,2,2trifluoroethyl) ether (BTFE) diluent into the NaFSI-based high concentration electrolyte to obtain a LHCE system with abundant AGG and CIP configurations. (Figure 9d) Manthiram et al.[72] reported that LHCE with TTE as the diluent can restrain the transition-metal dissolution and intragranular cracking of O₃type Na(Ni_{0.3}Fe_{0.4}Mn_{0.3})O₂ cathode. Wu et al.^[73] reported that in a diglyme-based LHCE system with 1,3-dioxolane as the diluent, Na+ coordinated solvent shows a lower HOMO level compared with free solvents and thus exhibits excellent oxidation stability up to 4.5 V. The aforementioned HCE and LHCE systems are used in ether systems, while a high concentration of ester electrolyte may have side effects on the formation of CEI. (Figure 9e) For example, Wang et al. [74] tuned CEI on high-voltage NVPF cathode by changing anion/solvent ratios in electrolytes (carbonate electrolyte with 3.0, 1.0, or 0.3 M NaClO₄, respectively). The results indicated that high anion/solvent ratio leads to CEI with more anion derivatives (C_xClO_y) which shows larger

16146840, 2025, 15, Downloaded from https://advanced.onlinelibrary.wiky.com/doi/10.1002/semm.202405301 by University Town Of Shenzhen, Wiley Online Library on [1711/2025]. See the Terms and Conditions (https://onlinelibrary.wiky.com/term/

conditions) on Wiley Online Library for rules of use; OA articles are governed by the applicable Creative Commons

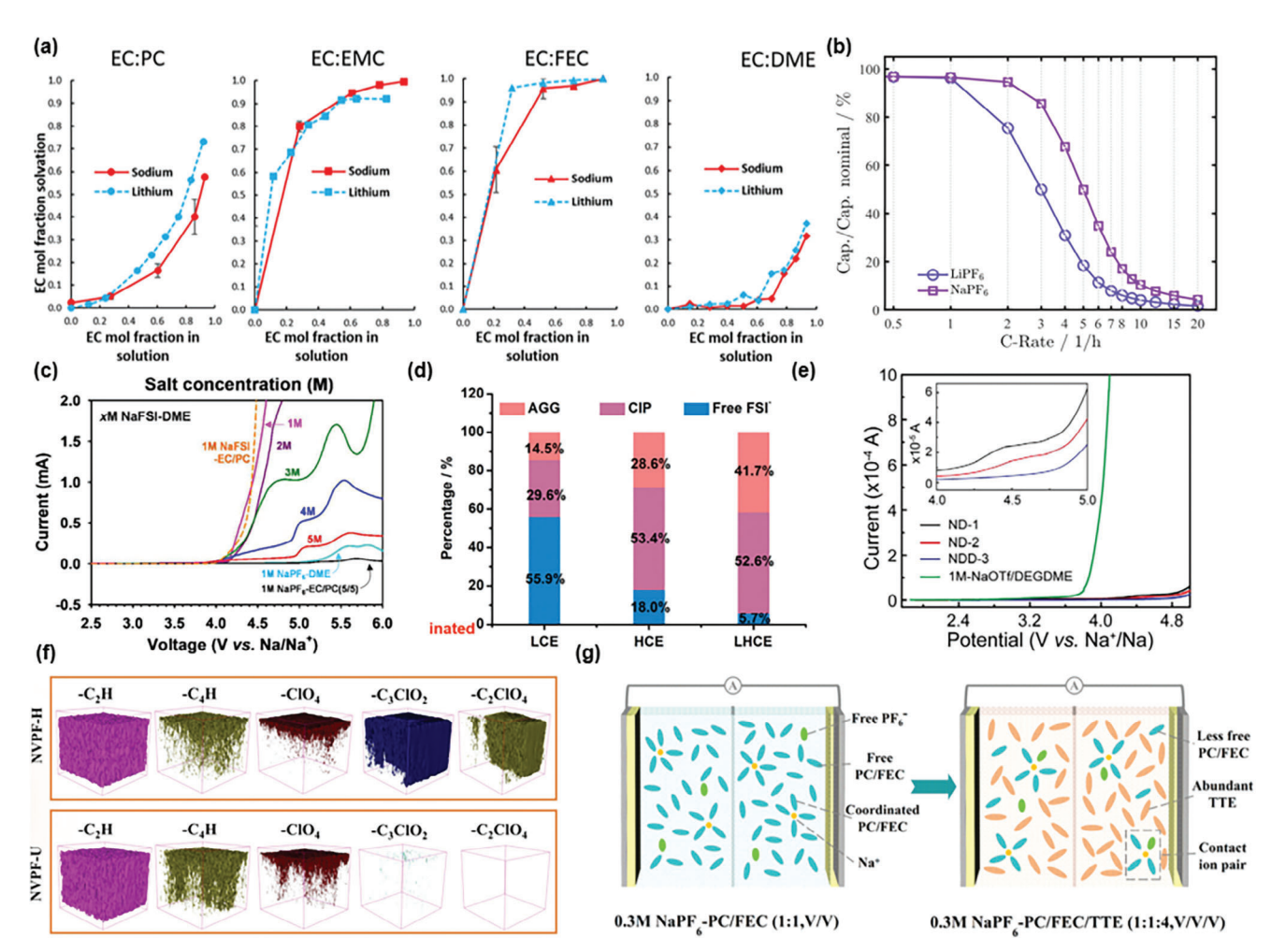


Figure 9. a) ESI-MS solvation analysis of Na⁺ in four electrolyte solutions shows similar solvation trends between Li⁺/Na⁺. Reproduced with permission.^[68] copyright 2017, Royal Society of Chemistry. b) Simulated discharge capacities at C-rates ranging from 0.5 C to 20 C with LiPF₆ and NaPF₆ in EC:DEC (1:1 v:v). Reproduced with permission.^[69] copyright 2021, IOP Publishing. c) Anodic limits of conventional dilute and highly concentrated electrolytes on an Al working electrode at a scan rate of 1 mVs⁻¹. Reproduced with permission.^[70] copyright 2017, American Chemical Society. d) Proportion of free FSI⁻, CIP, and AGG, free and Na⁺-coordinated DME. Reproduced with permission.^[71] copyright 2023, Wiley-VCH. e) LSV comparison of different electrolytes. Reproduced with permission.^[73] f) Spatial distribution of some representative ion fragments in the derived interphase on the NVPF cathodes. Reproduced with permission.^[74] copyright 2022, Wiley-VCH. g) Scheme of the solvation structure in the 0.3 M NaPF₆-PC/FEC (1:1, v/v) and 0.3 M NaPF₆-PC/FEC/TTE (1:1:4, v/v/v). Reproduced with permission.^[76] copyright 2023, American Chemical Society.

interfacial Na+ transport resistance and more serious gas evolution. Comparatively, a low anion/solvent ratio derives a stable anion-tuned interphase that enables better interfacial kinetics and cycle ability. (Figure 9f) Therefore, reducing the concentration seems to be a worthwhile solution for ester electrolytes considering the low concentrate electrolyte(LCE) reduces the overall cost of SIBs thus increasing their practicability in large-scale energy storage. [75] Some inert solvents commonly used in LHCE systems as diluents also have positive effects on the performance of low-concentration electrolytes. For example, Du et al. [76] designed a nonflammable low-concentration electrolyte consisting of only 0.3 M NaPF₆ in FEC/PC/TTE, the specific Na⁺ solvation sheath structure modulated by the non-solvent TTE enables a dense and thin CEI film to be formed on the surface of Na₄Co₃(PO₄)₂P₂O₇ cathode. Moreover, the oxidation stability of this electrolyte is also improved significantly thus the Na₄Co₃(PO₄)₂P₂O₇/Na cell exhibits good cycle stability even when charged to a high voltage of 4.7 V. (Figure 9g).

6.2. Weak Ion-Solvent Coordination Interaction

The use of weakly coordinated solvents is another effective means to regulate the solvation structure. Introducing electron-withdrawing groups (such as fluorine groups or trifluoromethyl) into the molecular structure can disperse the charge of the nucleophilic site as well as weaken the coordination strength between Na⁺ and anions. Zhang et al. [77] designed a low-solvation electrolyte aiming to construct a less soluble electrode—electrolyte interphase both on the cathode (NaNi $_{0.68}$ Mn $_{0.22}$ Co $_{0.1}$ O $_{2}$) and anode (HC). With low polarity solvent (tris (2,2,2-trifluoroethyl) phosphate, TFEP) being used, proper salt species and solvent/salt

16146849, 2025, 15, Dwnholaded from https://advanced onlinelibrary.wiely.com/doi/10.1002/aem.20.2045301 by University Town Of Shenzhen, Wiley Online Library on [17/11/1225], See the Terms and Conditions (https://onlinelibrary.viely.com/terms-and-conditions) on Wiley Online Library for rules of use; OA articles are governed by the applicable Creative Commons

www.advancedsciencenews.com

molar ratio are selected, and the electrolyte shows reduced free solvents and anion-rich solvation structure. The designed electrolyte enables >90% capacity retention for NaNi_{0.68}Mn_{0.22}Co_{0.1}O₂/HC full cell with this electrolyte demonstrates after 300 cycles when charged to 4.2 V. Besides, usage of solvents with lower solvation ability can lower the activation energy barrier thus facilitate the charge-transfer reactions.[16] Manthiram et al. introduced the NaNO₃ salt as a diluent which reduces the usage of expensive sodium bis(fluorosulfonyl)imide (NaFSI) and fluoroether diluents required in conventional LHCE systems. By employing TMP as the single solvent dissolved with 1.1 M NaFSI and 0.3 M NaNO₃, a non-flammable, cost-effective electrolyte was constructed which enables the stable cycle life of Na(Ni_{0.3}Fe_{0.4}Mn_{0.3})O₂/Na cells with a capacity retention of 80% over 500 cycles at 0.2 C. The NaNO₃ diluent molecule can subtly replace the TMP site in the Na-ion primary solvation shell thus facilities the construction of a compact CEI derived from the decomposition of the electrolyte salts.

The design principles and strategies for the solvation structure of electrolytes in high-voltage SIBs focus on optimizing ionsolvent interactions to enhance electrochemical stability, ionic conductivity, and electrode compatibility. Both the regulation of anions (using HCEs) and the adjustment of solvents (reducing solvent coordination) essentially aim to construct an inorganicrich interphase layer on the cathode surface. In addition to these methods, other strategies for optimizing the solvation structure of SIBs include the use of functionalized solvents and cosolvent systems, the introduction of ionic liquids, the design of hydrogen-bonding networks, the application of novel anion receptors, and the regulation of the dynamics of the solvation shell. These approaches can further enhance the stability under high voltage, ionic conductivity, and cycle life of SIBs. However, further research on the solvation structure of SIBs is still needed.

7. CEI Formation/Functional Additives

The additive strategy has been recognized as a cost-effective approach for enhancing the overall performance of LIBs.[78,79] Although research on additives for the cathode of SIBs is still in its early stages, this approach holds promise for tuning the structure and composition of the CEI film, thereby improving the overall performance of the battery system.

7.1. Fluorinated Additive

Fluorinated additives typically have lower LUMO energy levels, enabling them to be preferentially reduced at the anode and form an effective protective layer. [80-83] Notably, the protective effect of these additives at the anode also helps reduce harmful chemical reactions at the cathode interface. For instance, Choi et al.[84] observed that decomposition products from the Na metal electrode tend to undergo electrochemical decomposition at the cathode, leading to overcharge behavior at 3.2 and 4.1 V (Figure 10a). This issue can be mitigated by using FEC as an electrolyte additive, as the FEC-derived SEI on the Na metal effectively prevents DMC decomposition. Beyond its notable film-forming ability on the anodes of HC and Na metal, FEC also exerts a positive effect on high-voltage cathodes by contributing to the formation of a fluorine-rich CEI film. For example, Li et al. [85] demonstrated that FEC improves the Coulombic efficiency and long-term cycling stability of the Na_{0.67}Mn_{0.8}Cu_{0.1}Mg_{0.1}O₂ material as an electrolyte additive. Post-mortem analysis using gas chromatography flame ionization detector (GC-FID) and ion chromatography (IC) revealed that FEC not only helps maintain a protective SEI at the anode but also suppresses transition metal dissolution at the cathode. Chen et al.[86] similarly reported that an appropriate amount of FEC significantly suppressed PC solvent decomposition and aided in forming a NaF-rich protective layer on the cathode surface, which helped preserve the structural stability of the cathode material. Additionally, some fluorinated additives can form a dense CEI layer at the cathode interface, enhancing the oxidative stability of ether-based electrolytes. For instance, Li et al.[87] introduced a series of perfluorinated-anion additives that preferentially self-assemble into a protective CEI on the NVP cathode while concurrently creating a -C-F...H-C- stable interaction network to enhance the stability of diglyme (Figure 10b). Among them, sodium pentadecafluorooctanoate (SPFO) as an additive can restrain weak oxidation at low voltage and withstand high voltage up to 4.5 V versus Na/Na⁺ (Figure 10c).

7.2. Additives Containing Unsaturated Bonds

As early as 2011, Ohsawa compared a series of well-known film-forming organic electrolyte additives in LIBs, such as FEC, trans-difluoroethylene carbonate (DFEC), VC, and ethylene sulfite, identifying FEC as the only effective electrolyte additive for SIBs.^[88] However, this study was limited to ester-based electrolytes. In 2021, Chen et al. developed long-life sodiumion full cells using NaOTf (sodium trifluomethanesulfonate)diglyme electrolyte with the help of a VC additive. The HOMO level of VC is close to that of diglyme, allowing it to synergistically oxidize at the cathode interface, forming a continuous CEI film on the NVP@C cathode and improving the oxidative stability of the diglyme-based electrolyte (Figure 10d). Furthermore, VC can participate in the solvent sheath structure of Na+ by forming a Na+-VC complex, making the NaOTf-diglyme system well-matched with NVP@C.[89] Zhang et al.[90] combined VC with sulfolane as effective dual additives to stabilize PCbased electrolytes, achieving a capacity retention of 94% and a Coulombic efficiency of 99.9% over 600 cycles at 5 C for the NaNi_{0.68}Mn_{0.22}Co_{0.1}O₂/Na cell. The synergistic effect of these two additives enables the formation of a homogeneous, dense, and thin hybrid CEI consisting of F- and S-containing species on the surface of NaNi_{0.68}Mn_{0.22}Co_{0.1}O₂.

7.3. Anhydride

Certain anhydride molecules can form an effective CEI film on transition metal oxides cathodes. For example, Sun et al.[91] employed diglycolic anhydride (DGA) as a CEI-forming electrolyte additive to create a robust interface on Na_{0.67}Li_{0.2}Ni_{0.23}Mn_{0.67}O₂. DGA effectively inhibits electrolyte degradation caused by (O2)_n species (Figure 10f). With the addition of 2 wt.% DGA, the capacity retention of the Na_{0.67}Li_{0.2}Ni_{0.23}Mn_{0.67}O₂/Na system improved www.advancedsciencenews.com

1/1/10/25, 15, Dwnbaded from https://advanced on inhelibrary.wiely.com/doi/10/10/2acm.20/2405301 by University Town of Shenzhen, Wiley Online Library on [1/1/10/25], Se the Terms and Conditions (https://onlinelibrary.wiely.com/terms-and-conditions) on Wiley Online Library for rules of use; OA articles are governed by the applicable Creative Commons

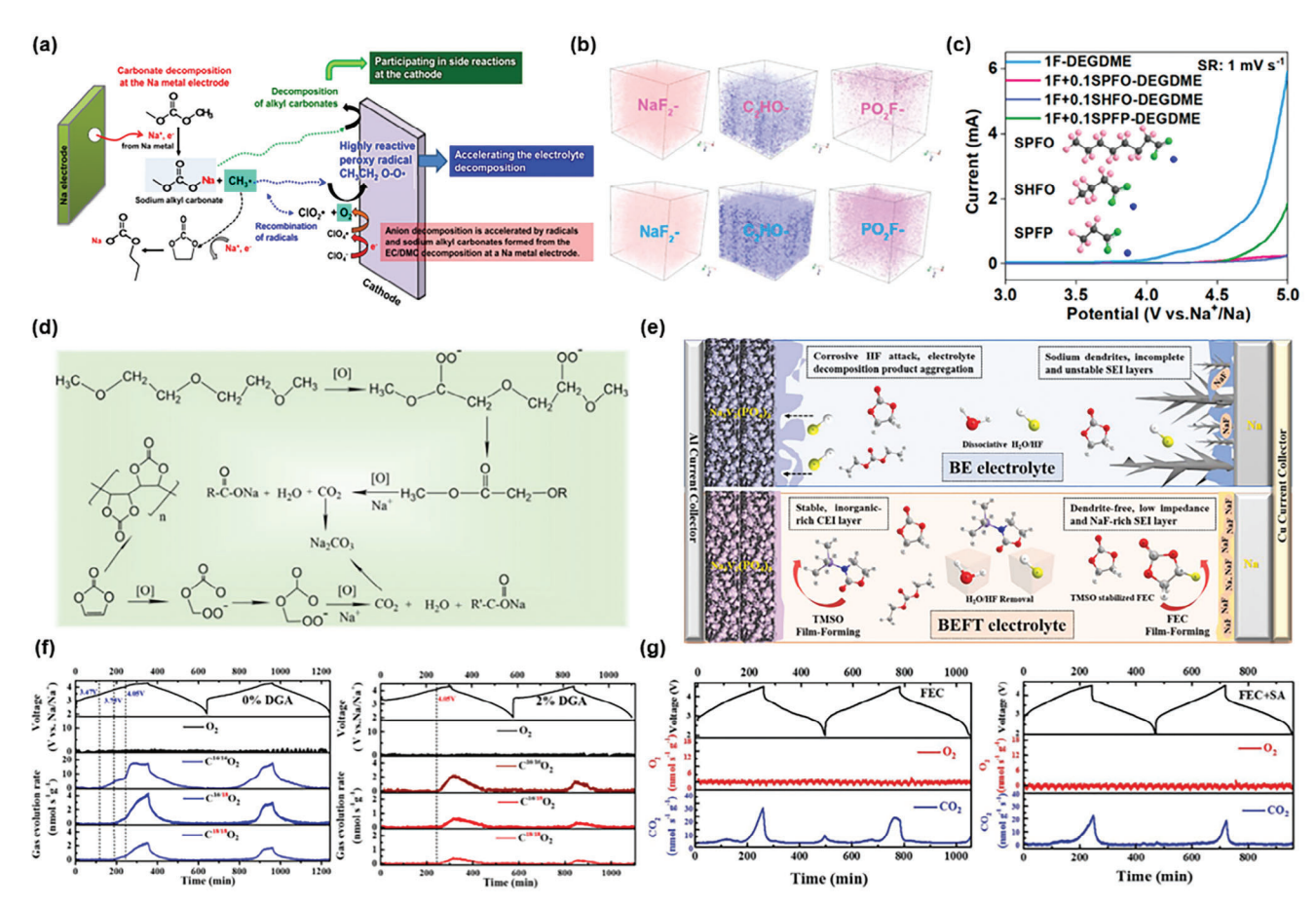


Figure 10. a) Schematic illustration of reduced anodic stability of electrolytes due to the decomposition of the linear carbonate DMC at the Na metal electrode. Réproduced with permission. [84] copyright 2016, Elsevier. b) TOF-SIMS spatial distribution visualization of SPFO-containing electrolyte and blank electrolyte after 10 cycles. Reproduced with permission.^[87] copyright 2024, American Chemical Society. c) LSV curves in 1 M NaPF₆-diglyme electrolytes with different additives from 3 to 5 V at a scanning rate of 1 mV s⁻¹. Reproduced with permission. (87) copyright 2024, American Chemical Society. d) The possible reaction equation during the oxidation process of VC. Reproduced with permission. [89] copyright 2021, Elsevier. e) Schematic illustration of the mechanism of silane additives on SIBs cathodes take TMSO as an example. Reproduced with permission. [95] copyright 2022, Elsevier. f) DEMS result of ¹⁸O isotope labeled cathode from the cell without DGA (Left) and the cell with DGA (Right) cycled at 0.2 C rate for two cycles. Reproduced with permission. [91] copyright 2023, Elsevier. g) DEMS test of the cell with FEC the cell with FEC and SA cycled at 0.2 C rate for two cycles. Reproduced with permission.^[92] copyright 2021, Wiley-VCH.

significantly from 1.6% to 92.59% after 1000 cycles at 1 C. In another study, Sun et al.[92] combined succinic anhydride (SA) and FEC as synergistic film-forming additives to enhance the cycling performance of $Na_{0.6}Li_{0.15}Ni_{0.15}Mn_{0.55}Cu_{0.15}O_2$. SA is expected to oxidize before FEC and PC in the electrolyte, forming a homogeneous CEI with more oxygen-rich organic species and less NaF. Additionally, online DEMS tests revealed that this dual-additive approach effectively suppresses CO₂ evolution (Figure 10g).

7.4. Silane

In carbonate-based electrolytes, corrosion is driven by the facile ring-opening polymerization induced by Lewis acids, particularly PF5. As demonstrated in LIBs studies, molecules containing Si-N or Si-O bonds can effectively trap HF species. By using trimethoxy(pentafluorophenyl)silane (TPFS) and NaClO₄ as dual additives, the cathode is stabilized in two key ways.^[93] First, ClO₄ strongly coordinates with Na⁺, forming stable polymerlike chains with the solvents. Second, TPFS participates in the solvation of the PF₆⁻ anion, suppressing the PF₆⁻-solvent interaction. Additionally, TPFS exhibits the ability to scavenge harmful HF and H2O species in the electrolyte, thereby initiating a self-purifying process. When the modified electrolyte (1 M NaPF₆ in EC/DEC with 0.2 wt.% NaClO₄ + 1 wt.% TPFS) was used in a Na₃V₂(PO₄)₂O₂F/Na cell, it achieved a capacity retention of 93% after 500 cycles and average Coulombic efficiency of 99.6% at 4.7 V. Xiang et al. developed a poly (VC)based quasi-solid polymer electrolyte containing N-methyl-N-(trimethylsilyl)trifluoroacetamide (MSTFA) as a multifunctional additive. MSTFA acts as an efficient plasticizer and HF/H₂O scavenger, thereby improving the ionic conduction of the electrolyte and suppressing the corrosion of free acid at the cathode. Consequently, the cycling stability of the Na|| NVPF cell under high voltage (up to 4.4 V) was significantly enhanced. [94] Yu et al. [95] utilized 3-Trimethylsilyl-2-oxazolidinone (TMSO) as a multifunctional additive, which not only inhibits the decomposition of NaPF₆ in FEC-containing electrolytes but also removes H₂O and

16146480, 2025, 15, Dwnholedef from https://dwnce.condinibilibrary.wiely.com/oi/01/002/acmn.202405301 by University Town of Sherazhen, Wiley Online Library on [1/1/1025]. See the Terms and Conditions (https://onlinelibrary.wiely.com/terms-and-conditions) on Wiley Online Library for rules of use; OA articles are governed by the applicable Creative Commons

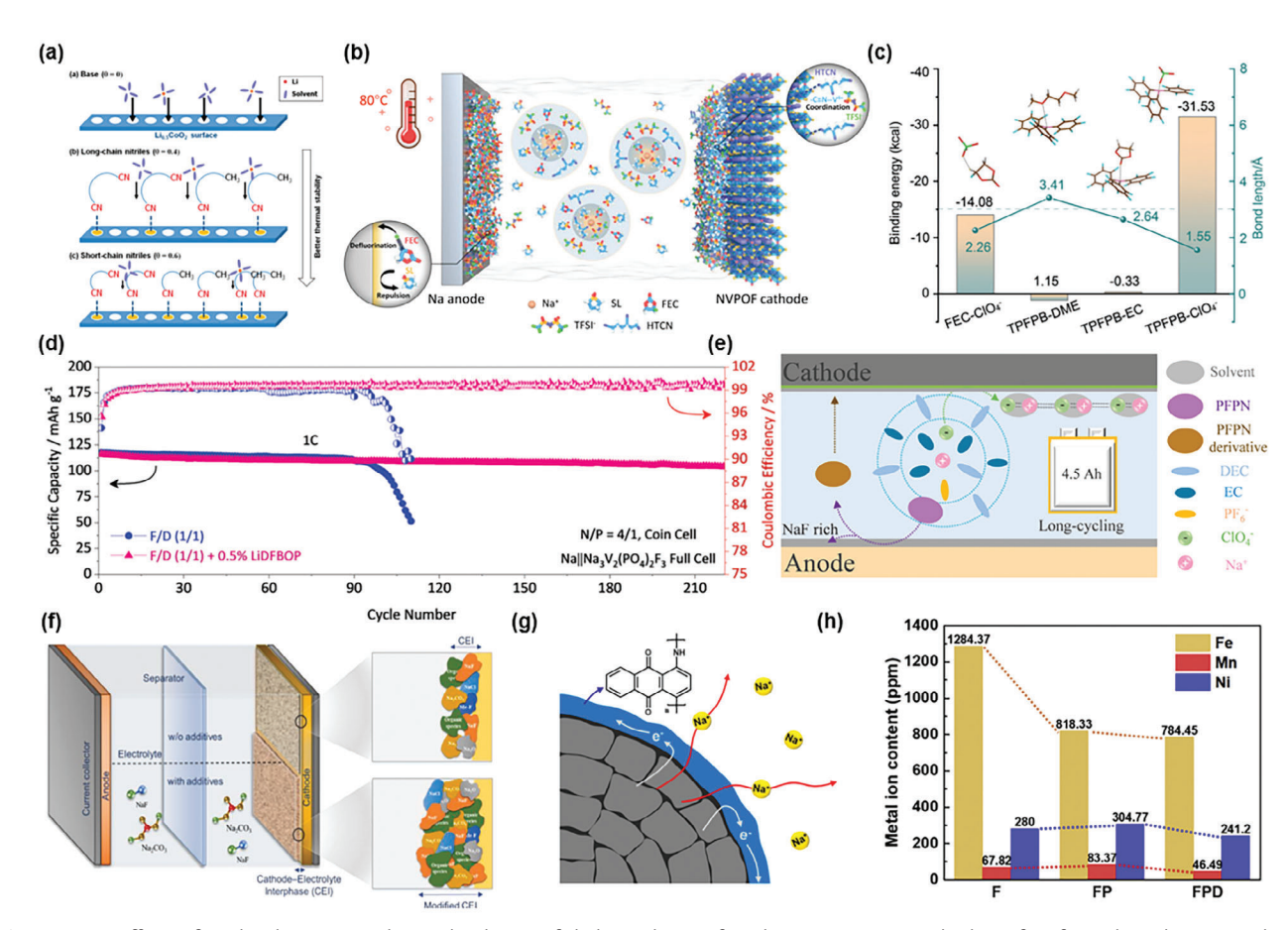


Figure 11. a) Effects of nitrile adsorption and steric hindrance of aliphatic chains of nitriles on protecting cathode surface from electrolyte. Reproduced with permission. [100] copyright 2017, American Chemical Society. b) Schematic illustration of the NVPOF/Na battery with the designed electrolyte. Reproduced with permission. [100] copyright 2022, American Chemical Society. c) Binding energy and bond length of FEC-CIO₄⁻, TPFPB-DME, TPFPB-EC, and TPFPB-CIO4⁻ through H—O, B—O, B—O, and B—O interactions, respectively. Reproduced with permission. [102] copyright 2024, Wiley-VCH. d) Cycling performance of NVPOF/Na battery operated in electrolyte with and without 0.5% LiDFBOP at 1 C. Reproduced with permission. [105] copyright 2022, Royal Society of Chemistry. e) Theoretical model of electrolyte with PFPN as the additive. Reproduced with permission. [106] copyright 2024, Elsevier. f) Images of the original CEI layer formed without additives and the modified CEI by Na₂CO₃ and NaF additive. Reproduced with permission. [107] copyright 2021, Elsevier. g) Schematic presentation for enhancing the electrochemical performance of the NVPF cathode by the formation of an electronically-conductive AAQ layer. Reproduced with permission. [109] copyright 2020, Elsevier. h) Effect of electrolyte additive on the dissolution of transition metal ions. Reproduced with permission. [108] copyright 2018, Elsevier.

HF from the electrolyte. Moreover, TMSO forms a robust CEI layer on the NVP cathode, mitigating cracking and structural pulverization. The functions of silane additives containing Si-N or Si-O bonds are summarized in Figure 10e.

7.5. Nitriles

Nitriles can modify the electrode/electrolyte interface by bonding to transition metal ions in the cathode material, participating in the formation of the CEI, and thereby suppressing thermally accelerated interfacial side reactions (**Figure 11a**). [96–98] For instance, Shu et al. [99] employed adiponitrile (ADN) as an additive to enhance the cycle stability of $Na_{0.76}Ni_{0.3}Fe_{0.4}Mn_{0.3}O_2$. Computational results indicate that ADN has a lower HOMO than carbonate solvents, making it more readily oxidized at the cathode, which promotes the formation of a more uniform and compact CEI. The $Na_{0.76}Ni_{0.3}Fe_{0.4}Mn_{0.3}O_2/HC$ full cell with an

electrolyte containing 3% ADN maintained 78% of its capacity after 220 cycles, whereas the capacity of the cell without ADN dropped rapidly to 75% after just 40 cycles. Huang et al. [100] introduced FEC and 1,3,6-hexanetricarbonitrile (HTCN) as cosolvents in a sulfolane-based electrolyte to construct robust interphases on both the Na anode and the Na $_3$ V $_2$ (PO $_4$) $_2$ O $_2$ F cathode (Figure 11b). Specifically, the three –C=N groups of HTCN effectively coordinate with the unoccupied orbitals of V $^{4+}$ ions in Na $_3$ V $_2$ (PO $_4$) $_2$ O $_2$ F, thereby stabilizing the cathode surface, further suppressing adverse parasitic reactions, and preventing CEI cracking during long-term cycling.

7.6. Boron-Containing Additive

NaDFOB can construct a robust borate and fluoride-rich interphase on the cathode through the preferential oxidation of DFOB⁻.^[99] For example, low-concentration electrolytes tend to

ADVANCED ENERGY MATERIALS 16146849, 2025, 15, Downloaded from https://advanced onlinelibrary.wiely.com/doi/10.002/aem.m.202405301 by University Town Of Shenzhen, Wiley Online Litary on [1711/12025]. See the Terms and Conditions (https://onlinelibrary.wiely.com/terms-and-conditions) on Wiley Online Library for rules of use; OA archies are governed by the applicable Centwise Commons I

form an organic-dominated interface derived from decomposed solvents within the SSIPs solvation structure. This organic-rich CEI is generally considered fragile and deficient for long-term cycling performance in SIBs. This issue can be mitigated by incorporating certain additives. For example, Meng et al.[101] utilized dual additives, NaDFOB and tris(trimethylsilyl)borate (TMSB), in an ultralow concentration electrolyte (0.3 M NaPF₆ in EC/PC) to construct robust interfacial films on both the $\text{NaNi}_{1/3}\text{Fe}_{1/3}\text{Mn}_{1/3}\text{O}_2$ cathode and HC anode. Besides ester-based electrolytes, NaDFOB also exhibits a synergistic film-forming effect in ether-based systems. For instance, Chou et al.[102] introduce the NaDFOB into diglyme electrolyte as additives to reinforce the CEI and promise interfacial stability of FeMnHCF FeMn-based Prussian blue cathode. The robust NaF and B-rich CEI pre-formed on FeMnHCF prevents undesirable oxidative decomposition of electrolyte as well as transition metal dissolution. Beyond film formation, some additives can also modulate the solvation structure. For instance, the electron-deficient boron (B) center in tris(pentafluorophenyl)borane (TPFPB) acts as an anion receptor, attracting ClO₄⁻ and reducing its proportion in the primary solvation sheath (Figure 11c). The oxidative stability of the TPFPB-containing electrolyte was significantly enhanced due to the reduced distribution of free solvents, enabling the NVP cathode to cycle under a high cut-off voltage of 4.2 V (vs Na⁺/Na) across a wide temperature range from −30 to 60 °C.[103]

7.7. Phosphorus-Containing Additive

Nan et al.[104] employed sodium difluorophosphate (NaDFP) as a dual-functional electrolyte additive to construct a highquality CEI on NaNi_{0.33}Fe_{0.33}Mn_{0.33}O₂ and optimize the solvation structure of Li⁺. Similarly, Xia et al.[105] reported a welltailored carbonate-based electrolyte containing lithium difluorobis(oxalato) phosphate (LiDFBOP) as a multifunctional additive. The DFBOP- anions form a stable and robust organic/inorganic hybrid interphase, effectively suppressing uncontrolled parasitic reactions. Additionally, Li⁺ ions participate in solvation, altering the redox stability of the basic electrolyte components. The assembled 4.5 V NVPF/Na cell exhibited 90% capacity retention after 220 cycles and achieved a high energy density of 295 Wh kg⁻¹ with limited Na (Figure 11d). Phosphorus-containing additives with flame-retardant properties also contribute positively to the construction of the cathode interphase. For example, Li et al.[106] proposed a dual-additive strategy using NaClO₄ and PFPN to create a double-layer CEI on the Na₃Fe₂(PO₄)P₂O₇ cathode. Initially, ClO₄ reaches the cathode surface, interacting with Na⁺ and solvents to form a NaCl and polymer-like chain CEI. Subsequently, PFPN derivatives migrate to the cathode surface, where they undergo ring opening and decomposition, leading to the formation of a stable double-layer CEI (Figure 11e).

7.8. Other Additives

In addition to the aforementioned organic additives, some inorganic sodium salts with specific structures are also used as electrolyte additives. For example, Chung et al. [107] build a thick and stable CEI layer on the Na $_{0.67}$ Fe $_{0.5}$ Mn $_{0.5}$ O $_2$ cathode with high contents of Na $_2$ CO $_3$ and NaF by applying these two components as

the electrolyte additives. According to the XAS, XPS, and TOF-SIMS analyses, the newly formed CEI layer could suppress the dissolution of transition metals into the electrolyte. (Figure 11f) Mitra et al. $^{[108]}$ add two high-donor salt anions (TFSI $^-$ and BF $_4$ $^-$) as additives in a conventional electrolyte system (1 M NaPF $_6$ EC:PC). The dual anion additives are able to participate in the inner solvation shell around the Na $^+$ and support the build of inorganic-rich CEI. As a result, the electrolyte with dual additives exhibits oxidative stability up to 4.5 V, simultaneously mitigating the undesired side reactions at high voltage operation of the layered sodium nickel manganese oxide cathode.

Additionally, some additives can undergo in situ polymerization on the cathode surface. Kim et al. [109] developed 1-aminoanthraquinone (AAQ) as an electro-polymerizable additive in liquid electrolytes. By adding 0.06 wt.% AAQ, an in situ formed polymer layer was created, providing an effective conduction pathway in the NVPF electrode. This layer enhanced cycling performance, including discharge capacity, cycling stability, and rate capability. (Figure 11g).

7.9. Multiple Additive Synergistic Effect

Although the above additives have demonstrated unique properties, none can fully meet the requirements of high-voltage cathodes for SIBs. Therefore, combining multiple types of additives is a practical strategy to further enhance the overall performance of the battery. For example, using FEC in combination with two sulfur-containing molecules, dioxathiolane-2,2-dioxide (DTD) and prop-1-ene-1,3-sultone (PST), as a triadditive, effectively suppresses the dissolution of transition metals in NaNi_{1/3}Fe_{1/3}Mn_{1/3}O₂ by forming a dense and thick CEI on the cathode. (Figure 11h) The capacity retention of 1 Ah NaNi_{1/3}Fe_{1/3}Mn_{1/3}O₂/HC pouch cell reaches 92.2% after 1000 cycles at 1C.[35] A significant feature of sulfur-containing additives, such as sulfites, sulfates, and sultones, is their excellent compatibility with VC, resulting in superior performance compared to using either additive alone. [110,111] Tarascon et al. [112] designed an electrolyte with four additives: VC, succinonitrile (SN), 1,3-propane sultone (1,3-PS), and NaDFOB. These additives work synergistically to produce a NaF film, thin elastomers, and sulfate-based deposits, thereby constructing a stable SEI at both the negative and positive electrodes in a NVPF/C cell. The 18 650 Na-ion batteries cycled with this optimized electrolyte display impressive high-temperature performance (55 °C). The use of sulfur-based additives such as 1,3-PS and DTD effectively mitigates electrolyte oxidation during cycling, enabling Na(Ni_{0.4}Mn_{0.4}Cu_{0.1}Ti_{0.1})_{0.999}La_{0.001}O₂/HC full cells to operate within a voltage range of 1.2–4.4 V.[113]

Among all existing electrolyte design strategies, the use of tailored electrolyte additives is the most simple, scalable, and economical method to modify the CEI of SIBs. The additives used for high-voltage sodium battery cathodes and their functions are summarized in **Figure 12** below. It is not hard to find that Most additives used in the SIBs are derived from tests conducted in lithium-based systems. However, not all additive formulations that are effective in LIBs can be directly applied to SIBs. For example, combining DFEC with FEC as additives has been shown to improve the cyclability of $\text{Li}_{1.2}\text{Mn}_{0.56}\text{Co}_{0.08}\text{Ni}_{0.16}\text{O}_{2}$, [114] yet this

16146840, 2025, 15, Downloaded from https://advancec

com/doi/10.1002/aemm.202405301 by University Town Of Shenzhen, Wiley Online Library on [17/11/2025]. See the Terms and Conditions (https://onlinelibrary.wiley.com/terms/

and-conditions) on Wiley Online Library for rules of use; OA articles are governed by the applicable Creative Commons

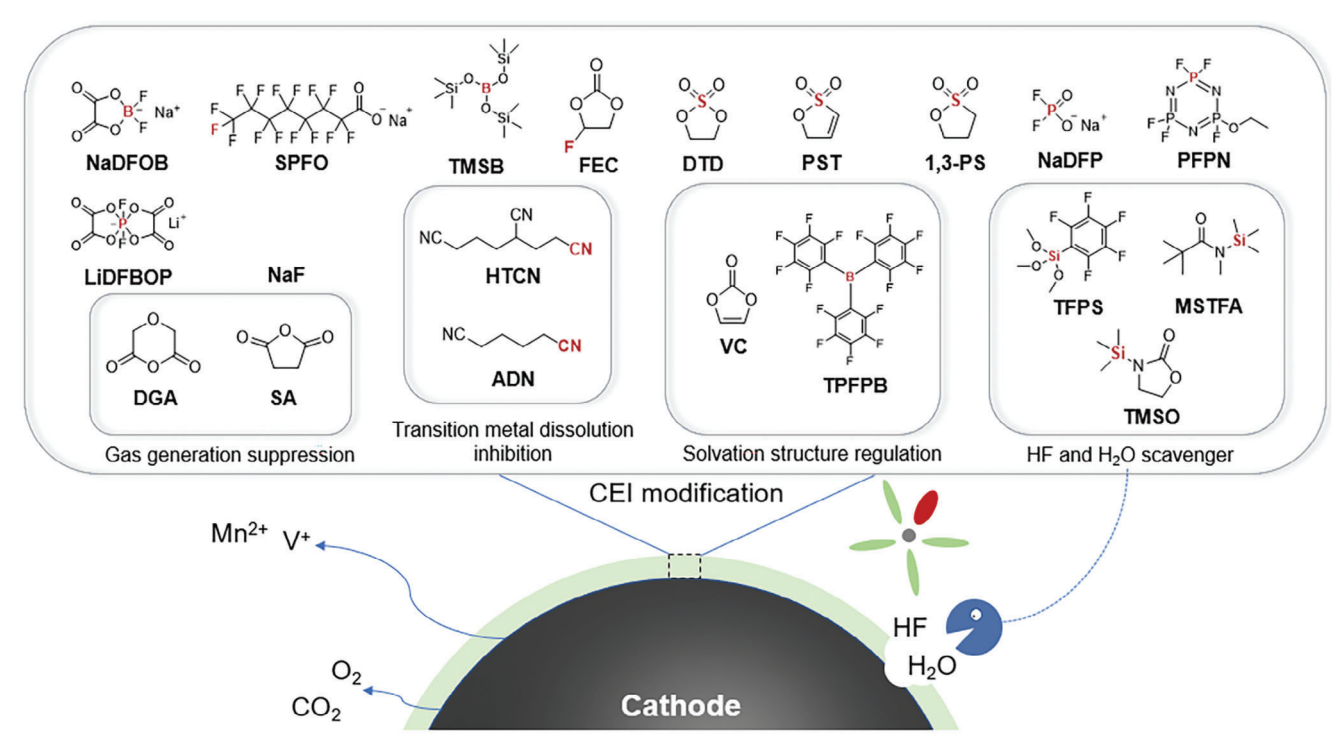


Figure 12. Schematic diagram of interface improvement by additives and classification of additive functions.

strategy appears to be detrimental to the performance of cathodes when used in SIB electrolytes. [115] Additionally, it is important to note that the use of multiple additives significantly increases the complexity of the electrolyte system. The inefficiency of trial-and-error approaches, along with the limitations of theoretical calculations, highlights the need for high-throughput screening and machine learning to identify synergistic additive combinations.

8. Conclusion and Perspectives

In this review, we provide a comprehensive overview of the latest advancements in cathode materials for SIBs, offering an in-depth analysis of how interfacial chemistry affects electrochemical performance. The chemical, structural, and electrochemical degradation processes, from the bulk to the surface of cathode materials, are fundamentally linked to the cathode-electrolyte interface. In other words, the stability and integrity of this interface during cycling are critical to the overall battery efficiency. As the operating voltage increases, the demands on a sable and robust CEI become more stringent. For example, at high voltages, cathode materials can experience significant volume changes and transition metal dissolution, which are often accompanied by repeated rupture and regeneration of the CEI film.

Recent research has led to notable advancements in improving sodium storage performance in cathode materials. A better understanding of additive mechanisms, solvation structure evolution, and the decomposition pathways of solvents and salts has facilitated the design of high-voltage stable electrolytes and enabled the construction of more robust CEI layers. However, the development of new electrolytes and the study of cathode interfaces remain largely dependent on time-consuming trial-and-

error approaches. Additionally, much of the existing literature lacks systematic analysis and interdisciplinary integration. Consequently, the evolution of the CEI, particularly at high voltages, remains unclear and requires further investigation. Beyond the challenges posed by high-voltage operation, recent advancements such as multi-additive synergistic strategies and high-entropy approaches have introduced additional complexity to the study of cathode interface formation and evolution. Decoupling the intricate chemical and electrochemical reactions at the interface, especially in systems with multiple components, remains a significant challenge. It appears that electrolyte development often lags behind cathode material advancements, while the progress in interface characterization techniques lags behind both. To address these issues and accelerate the commercialization of high-voltage SIBs, we propose the following perspectives on electrolyte design for constructing a stable cathode interface:

1) Electrolyte research requires a new paradigm to accelerate the pace of innovation and iteration. Artificial intelligence (AI) plays a transformative role in battery electrolyte research by accelerating the discovery and optimization of novel electrolyte materials. Machine learning algorithms analyze large datasets to predict the electrochemical performance of new electrolyte formulations, reducing the need for extensive trial-and-error experimentation. AI models can also optimize electrolyte compatibility with various electrode materials, ensuring stable interfaces and improved performance. Additionally, AI-driven simulations and predictive algorithms help in understanding degradation mechanisms and optimizing electrolyte formulations for enhanced safety, stability, and efficiency. Therefore, the integration of AI can significantly

www.advenergymat.de

- shorten development cycles and advance next-generation battery technologies.
- 2) Given the increasing complexity of electrolyte components (including three or more mixed solvents, solutes, and additives) and electrode materials (involving doping and coatings with multiple elements), in situ and operando analyses are essential for probing interfacial reactions between electrolytes and electrodes. These techniques are crucial for linking electrochemical performance observed in half-cells with that in full-cells.
- 3) Finally, considering the competitive advantages of SIBs over LIBs, particularly in large-scale energy storage applications, it is crucial to prioritize the cost-effectiveness and economic feasibility of electrolyte materials while simultaneously enhancing operating voltage and energy density. A practical approach for designing SIB electrolytes involves utilizing raw materials that are industrially scalable and minimizing electrolyte concentration where possible.
- 4) Solid-state electrolytes present unique advantages in high-voltage sodium-ion batteries, including a high oxidation potential and the ability to prevent the dissolution of transition metals in the cathode while suppressing the growth of sodium dendrites in the anode. However, the development of solid-state sodium-ion batteries remains in its early stages due to challenges such as high costs, complex fabrication processes, and poor interfacial contact. With continued research and a deeper understanding of interfacial issues, breakthroughs in solid-state sodium-ion batteries are anticipated.

As sodium-ion battery research advances, researchers will gain a deeper understanding of the sources of interface instability under high voltage, which will be beneficial for guiding the improvement of existing electrolytes and the development of new electrolyte materials. We believe that by continuously enhancing performance indicators, such as energy density, while maintaining the cost-effectiveness of sodium-ion batteries, they will eventually become a crucial component of future energy storage systems.

Conflict of Interest

The authors declare no conflict of interest.

Keywords

characterization techniques, electrolyte, high-voltage cathode, sodium-ion batteries

Received: November 13, 2024 Revised: December 12, 2024 Published online: January 2, 2025

- [1] Z. P. Cano, D. Banham, S. Ye, A. Hintennach, J. Lu, M. Fowler, Z. Chen, Nat. Energy 2018, 3, 279.
- [2] P. K. Nayak, L. T. Yang, W. Brehm, P. Adelhelm, Angew. Chem., Int. Ed. 2018, 57, 102.
- [3] S. P. Ong, V. L. Chevrier, G. Hautier, A. Jain, C. Moore, S. Kim, X. H. Ma, G. Ceder, Energy Environ. Sci. 2011, 4, 3680.

- [4] Q. Liu, Z. Hu, W. Li, C. Zou, H. Jin, S. Wang, S. Chou, S.-X. Dou, Energy Environ. Sci. 2021, 14, 158.
- [5] P. Barpanda, L. Lander, S.-i. Nishimura, A. Yamada, Adv. Energy Mater. 2018, 8, 1703055.
- [6] T. Yuan, Y. Chen, X. Gao, R. Xu, Z. Zhang, X. Chen, L. Cui, Small Methods 2023, 8, 2301372.
- [7] C. Fang, Y. Huang, W. Zhang, J. Han, Z. Deng, Y. Cao, H. Yang, Adv. Energy Mater. 2016, 6, 1501727.
- [8] Y. Chen, M. Yang, L. Yang, Z. Chen, H. Li, H. J. Woo, S.-S. Chi, Y. Xiao, J. Wang, C. Wang, Y. Deng, Chin. J. Struct. Chem. 2023, 42, 100028.
- [9] T. Song, E. Kendrick, J. Phys. Mater. 2021, 4, 032004.
- [10] Y. Wang, C. Xu, X. Tian, S. Wang, Y. Zhao, Chin. J. Struct. Chem. 2023, 42, 100167.
- [11] X. Han, Z. Liu, X. Hu, Q. Huang, D. Zhang, H. Guo, Q. Yi, Adv. Energy Sustain. Res. 2023, 5, 2300166.
- [12] P. Desai, J. Forero-Saboya, V. Meunier, G. Rousse, M. Deschamps, A. M. Abakumov, J. M. Tarascon, S. Mariyappan, *Energy Storage Mater.* 2023, 57, 102.
- [13] E. H. Wang, Y. B. Niu, Y. X. Yin, Y. G. Guo, ACS Mater. Lett. 2021, 3, 18.
- [14] E. Peled, S. Menkin, J. Electrochem. Soc. 2017, 164, A1703.
- [15] S. Janakiraman, A. Surendran, R. Biswal, S. Ghosh, S. Anandhan, A. Venimadhav, J. Electroanal. Chem. 2019, 833, 411.
- [16] L. Deng, K. Goh, F. D. Yu, Y. Xia, Y. S. Jiang, W. Ke, Y. Han, L. F. Que, J. Zhou, Z. B. Wang, Energy Storage Mater. 2022, 44, 82.
- [17] G.-L. Xu, R. Amine, A. Abouimrane, H. Che, M. Dahbi, Z.-F. Ma, I. Saadoune, J. Alami, W. L. Mattis, F. Pan, Z. Chen, K. Amine, Adv. Energy Mater. 2018, 8, 1702403.
- [18] L. Cheng, R. S. Assary, X. H. Qu, A. Jain, S. P. Ong, N. N. Rajput, K. Persson, L. A. Curtiss, J. Phys. Chem. Lett. 2015, 6, 283.
- [19] J. Huang, X. Han, F. Liu, C. Gervillie, L. A. Blanquer, T. Guo, J.-M. Tarascon, Energy Environ. Sci. 2021, 14, 6464.
- [20] J. Huang, L. A. Blanquer, J. Bonefacino, E. R. Logan, D. A. Dalla Corte, C. Delacourt, B. M. Gallant, S. T. Boles, J. R. Dahn, H.-Y. Tam, J.-M. Tarascon, Nat. Energy 2020, 5, 674.
- [21] J. Huang, C. Delacourt, P. Desai, C. Gervillie-Mouravieff, L. A. Blanquer, R. Tan, J.-M. Tarascon, J. Electrochem. Soc. 2023, 170, 090510
- [22] P. Desai, J. Huang, H. Hijazi, L. Zhang, S. Mariyappan, J.-M. Tarascon, Adv. Energy Mater. 2021, 11, 2101490.
- [23] C. Gervillie-Mouravieff, C. Boussard-Pledel, J. Huang, C. Leau, L. A. Blanquer, M. Ben Yahia, M. L. Doublet, S. T. Boles, X. H. Zhang, J. L. Adam, J. M. Tarascon, *Nat. Energy* 2022, 7, 1157.
- [24] E. Bendadesse, C. Gervillie-Mouravieff, C. Leau, K. Goloviznina, F. Rabuel, M. Salanne, J.-M. Tarascon, O. Sel, Adv. Energy Mater. 2023, 13
- [25] L. Sun, Z. Wu, M. Hou, Y. Ni, H. Sun, P. Jiao, H. Li, W. Zhang, L. Zhang, K. Zhang, F. Cheng, J. Chen, *Energy Environ. Sci.* 2023, 17, 210
- [26] K. Xu, Nat. Energy 2021, 6, 763.
- [27] A. Ponrouch, E. Marchante, M. Courty, J. M. Tarascon, M. R. Palacín, Energy Environ. Sci. 2012, 5, 8572.
- [28] J. Y. Jang, H. Kim, Y. Lee, K. T. Lee, K. Kang, N. S. Choi, *Electrochem. Commun.* 2014, 44, 74.
- [29] A. Ponrouch, R. Dedryvère, D. Monti, A. E. Demet, J. M. A. Mba, L. Croguennec, C. Masquelier, P. Johansson, M. R. Palacín, *Energy Environ. Sci.* 2013, 6, 2361.
- [30] D. Monti, E. Jonsson, A. Boschin, M. R. Palacin, A. Ponrouch, P. Johansson, Phys. Chem. Chem. Phys. 2020, 22, 22768.
- [31] J. L. Tebbe, T. F. Fuerst, C. B. Musgrave, ACS Appl. Mater. Interfaces 2016, 8, 26664.
- [32] L. D. Xing, O. Borodin, Phys. Chem. Chem. Phys. 2012, 14, 12838.
- [33] L. Yang, B. Ravdel, B. L. Lucht, Electrochem. Solid-State Lett. 2010, 13, A95.
- [34] T. Zhang, E. Paillard, Front. Chem. Sci. Eng. 2018, 12, 577.

ons) on Wiley Online Library for rules of use; OA articles are governed by the applicable Creative Common

- [35] H. Y. Che, X. R. Yang, H. Wang, X. Z. Liao, S. S. Zhang, C. S. Wang, Z. F. Ma, J. Power Sources. 2018, 407, 173.
- [36] H. Y. Che, X. R. Yang, Y. Yu, C. L. Pan, H. Wang, Y. H. Deng, L. S. Li, Z. F. Ma, Green Energy Environ. 2021, 6, 212.
- [37] G. C. Yan, D. Alves-Dalla-Corte, W. Yin, N. Madern, G. Gachot, J. M. Tarascon, J. Electrochem. Soc. 2018, 165, A1222.
- [38] X. X. Zhao, Z. Y. Gu, J. Z. Guo, X. T. Wang, H. J. Liang, D. Xie, W. H. Li, W. Q. Jia, X. L. Wu, Energy Environ. Mater. 2023, 6, e2474
- [39] J. R. He, T. Tao, F. Yang, Z. P. Sun, ChemSusChem 2022, 15, 202200480.
- [40] X. F. Guo, Z. Yang, Y. F. Zhu, X. H. Liu, X. X. He, L. Li, Y. Qiao, S. L. Chou, Small Methods 2022, 6, 2200209.
- [41] I. Hasa, S. Passerini, J. Hassoun, RSC Adv. 2015, 5, 48928.
- [42] S. Wu, B. Su, K. Ni, F. Pan, C. Wang, K. Zhang, D. Y. W. Yu, Y. Zhu, W. Zhang, Adv. Energy Mater. 2021, 11, 2002737.
- [43] D. Ba, Q. Gui, W. Liu, Z. Wang, Y. Li, J. Liu, Nano Energy 2022, 94, 106918.
- [44] L. Yin, M. Wang, C. Xie, C. Yang, J. Han, Y. Ya, ACS Appl. Mater. Interfaces 2023, 15, 9517.
- [45] Y.-Q. Zheng, M.-Y. Sun, F.-D. Yu, L. Deng, Y. Xia, Y.-S. Jiang, L.-F. Que, L. Zhao, Z.-B. Wang, *Nano Energy* **2022**, *102*, 107693.
- [46] M. M. Krishna, G. Jayasree, R. R. Mallu, P. Basak, ACS Appl. Energy Mater. 2023, 6, 9287.
- [47] M. Zhu, X. Zheng, L. Li, X. Zhu, Z. Huang, G. Wang, Y. Zhang, H. Liu, F. Yu, L. Wen, H.-K. Liu, S.-X. Dou, C. Wu, Energy Storage Mater. 2022, 48, 466.
- [48] S.-M. Oh, S.-T. Myung, C. S. Yoon, J. Lu, J. Hassoun, B. Scrosati, K. Amine, Y.-K. Sun, Nano Lett. 2014, 14, 1620.
- [49] J. Wang, Y. Yamada, K. Sodeyama, E. Watanabe, K. Takada, Y. Tateyama, A. Yamada, Nat. Energy 2018, 3, 22.
- [50] Z. Zeng, X. Jiang, R. Li, D. Yuan, X. Ai, H. Yang, Y. Cao, Adv. Sci. 2016, 3, 1600066.
- [51] X. Liu, X. Jiang, F. Zhong, X. Feng, W. Chen, X. Ai, H. Yang, Y. Cao, ACS Appl. Mater. Interfaces 2019, 11, 27833.
- [52] K. Du, C. Wang, P. Balaya, S. R. Gajjela, M. Law, Chem. Commun. 2022, 58, 533.
- [53] Y. Ma, B. Qin, X. Du, G. Xu, D. Wang, J. Wang, J. Zhang, J. Zhao, Z. Su, G. Cui, ACS Appl. Mater. Interfaces 2022, 14, 17444.
- [54] R. Mogensen, S. Colbin, A. S. Menon, E. Bjorklund, R. Younesi, ACS Appl. Energy Mater. 2020, 3, 4974.
- [55] M. Ma, B. Chen, X. Yang, Y. Liu, S. Dai, X. Qi, Y.-S. Hu, H. Pan, ACS Energy Lett. 2023, 8, 477.
- [56] Y. Jin, Y. Xu, B. Xiao, M. H. Engelhard, R. Yi, T. D. Vo, B. E. Matthews, X. Li, C. Wang, P. M. L. Le, J.-G. Zhang, Adv. Funct. Mater. 2022, 32.
- [57] H. Li, H. Chen, X. Shen, X. Liu, Y. Fang, F. Zhong, X. Ai, H. Yang, Y. Cao, ACS Appl. Mater. Interfaces 2022, 14, 43387.
- [58] X. Y. Jiang, X. W. Liu, Z. Q. Zeng, L. F. Xiao, X. P. Ai, H. X. Yang, Y. L. Cao, iScience 2018, 10, 114.
- [59] H. Che, S. Chen, Y. Xie, H. Wang, K. Amine, X.-Z. Liao, Z.-F. Ma, Energy Environ. Sci. 2017, 10, 1075.
- [60] S. M. Wang, C. L. Li, X. Q. Fan, S. X. Wen, H. L. Lu, H. Dong, J. Wang, Y. Quan, S. Y. Li, Energy Technol. 2021, 9, 2100190.
- [61] J. Chen, Z. G. Huang, C. Y. Wang, S. Porter, B. F. Wang, W. Lie, H. K. Liu, Chem. Commun. 2015, 51, 9809.
- [62] Z. F. Sun, W. B. Fu, M. Z. Liu, P. L. Lu, E. B. Zhao, A. Magasinski, L. Mengting, S. R. Luo, J. McDaniel, G. Yushin, J. Mater. Chem. A. 2020, 8, 4091.
- [63] J. Zhang, J. Li, G. Jia, H. Wang, M. Wang, Sustainable Energy Fuels 2024, 8, 2461.
- [64] D. M. C. Ould, S. Menkin, H. E. Smith, V. Riesgo-Gonzalez, E. Jonsson, C. A. O'Keefe, F. Coowar, J. Barker, A. D. Bond, C. P. Grey, D. S. Wright, Angew. Chem., Int. Ed. 2022, 61, 202202133.

- [65] A. J. Fernandez-Ropero, M. Zarrabeitia, G. Baraldi, M. Echeverria, T. Rojo, M. Armand, D. Shanmukaraj, ACS Appl. Mater. Interfaces 2021, 13, 11814.
- [66] C. L. Jiang, Y. Fang, W. Y. Zhang, X. H. Song, J. H. Lang, L. Shi, Y. B. Tang, Angew. Chem., Int. Ed. 2018, 57, 16370.
- [67] K. Xu, Chem. Rev 2004, 104, 4303.
- [68] A. V. Cresce, S. M. Russell, O. Borodin, J. A. Allen, M. A. Schroeder, M. Dai, J. Peng, M. P. Gobet, S. G. Greenbaum, R. E. Rogers, K. Xu, Phys. Chem. Chem. Phys. 2017, 19, 574.
- [69] J. Landesfeind, T. Hosaka, M. Graf, K. Kubota, S. Komaba, H. A. Gasteiger, J. Electrochem. Soc. 2021, 168, 040538.
- [70] J. Lee, Y. Lee, J. Lee, S. M. Lee, J. H. Choi, H. Kim, M. S. Kwon, K. Kang, K. T. Lee, N. S. Choi, ACS Appl. Mater. Interfaces 2017, 9, 3723.
- [71] J. H. Yu, W. C. Ren, C. Yu, Z. Wang, Y. Y. Xie, J. S. Qiu, Energy Environ. Mater. 2023. 6. e12602.
- [72] J. Lamb, A. Manthiram, ACS Appl. Mater. Interfaces 2022, 14, 28865.
- [73] H.-J. Liang, Z.-Y. Gu, X.-X. Zhao, J.-Z. Guo, J.-L. Yang, W.-H. Li, B. Li, Z.-M. Liu, W.-L. Li, X.-L. Wu, Angew. Chem., Int. Ed. 2021, 60, 26837.
- [74] L. Deng, F.-D. Yu, G. Sun, Y. Xia, Y.-S. Jiang, Y.-Q. Zheng, M.-Y. Sun, L.-F. Que, L. Zhao, Z.-B. Wang, Angew. Chem., Int. Ed. 2022, 61, 107693.
- [75] Y. Li, Y. Yang, Y. Lu, Q. Zhou, X. Qi, Q. Meng, X. Rong, L. Chen, Y.-S. Hu, ACS Energy Lett. 2020, 5, 1156.
- [76] J. Y. Zeng, D. C. Guan, W. G. Wang, X. Tan, Y. B. Cao, Z. D. Peng, G. R. Hu, K. Du, ACS Appl. Energy Mater. 2023, 6, 4238.
- [77] Y. Jin, P. M. L. Le, P. Gao, Y. Xu, B. Xiao, M. H. Engelhard, X. Cao, T. D. Vo, J. Hu, L. Zhong, B. E. Matthews, R. Yi, C. Wang, X. Li, J. Liu, J.-G. Zhang, Nat. Energy 2022, 7, 718.
- [78] A. M. Haregewoin, A. S. Wotango, B.-J. Hwang, Energy Environ. Sci. 2016. 9, 1955.
- [79] M. Wang, Q. Sun, Y. Liu, Z. Yan, Q. Xu, Y. Wu, T. Cheng, Chin. J. Struct. Chem. 2024, 42, 43.
- [80] D. Q. Liu, K. Qian, Y. B. He, D. Luo, H. Li, M. Y. Wu, F. Y. Kang, B. H. Li, Electrochim. Acta. 2018, 269, 378.
- [81] L. L. Liu, S. L. Wang, Z. Y. Zhang, J. T. Fan, W. Qi, S. M. Chen, *Ionics* 2019. 25, 1035.
- [82] E. Markevich, G. Salitra, K. Fridman, R. Sharabi, G. Gershinsky, A. Garsuch, G. Semrau, M. A. Schmidt, D. Aurbach, *Langmuir* 2014, 30, 7414.
- [83] L. Wang, Y. L. Ma, Y. T. Qu, X. Q. Cheng, P. J. Zuo, C. Y. Du, Y. Z. Gao, G. P. Yin, Electrochim. Acta. 2016, 191, 8.
- [84] Y. Lee, J. Lee, H. Kim, K. Kang, N. S. Choi, J. Power Sources. 2016, 320, 49.
- [85] J. Li, J. Wang, X. He, L. Zhang, A. Senyshyn, B. Yan, M. Muehlbauer, X. Cao, B. Vortmann-Westhoven, V. Kraft, H. Liu, C. Luerenbaum, G. Schumacher, E. Paillard, M. Winter, J. Li, J. Power Sources. 2019, 416, 184.
- [86] Z. J. Cheng, Y. Y. Mao, Q. Y. Dong, F. Jin, Y. B. Shen, L. W. Chen, Acta Phys. -Chim. 2019, 35, 868.
- [87] X. Hou, T. Y. Li, Y. L. Qiu, M. Q. Jiang, H. Z. Lin, Q. Zheng, X. F. Li, ACS Energy Lett. 2024, 9, 461.
- [88] S. Komaba, T. Ishikawa, N. Yabuuchi, W. Murata, A. Ito, Y. Ohsawa, ACS Appl. Mater. Interfaces 2011, 3, 4165.
- [89] J. Shi, L. N. Ding, Y. H. Wan, L. W. Mi, L. J. Chen, D. Yang, Y. X. Hu, W. H. Chen, J. Energy Chem. 2021, 57, 650.
- [90] P. M. L. Le, T. D. Vo, K. M. Le, T. N. Tran, Y. B. Xu, A. L. Phan, L. T. M. Le, H. V. Nguyen, B. W. Xiao, X. L. Li, Y. Jin, M. H. Engelhard, P. Y. Gao, C. M. Wang, J. G. Zhang, Small 2024, 20, 2402256.
- [91] P. Dai, C.-G. Shi, Z. Huang, X.-H. Wu, Y.-P. Deng, J. Fu, Y. Xie, J. Fan, S. Shen, C.-H. Shen, Y. Hong, G. Li, Y. Wen, Z. Chen, L. Huang, S.-G. Sun, Energy Storage Mater. 2023, 56, 551.
- [92] J.-J. Fan, P. Dai, C.-G. Shi, Y. Wen, C.-X. Luo, J. Yang, C. Song, L. Huang, S.-G. Sun, Adv. Funct. Mater. 2021, 31, 2010500.

16146840, 2025, 15, Downloaded from https://advanced.onlinelibrary.wiley.com/doi/10.1002/nemm.202405301 by University Town Of Shenzhen, Wiley Online Library on [17/11/2025]. See the Terms

and Conditions (https://onlinelibrary.wiley.com/term

and-conditions) on Wiley Online Library for rules of use; OA articles are governed by the applicable Creative Common

www.advenergymat.de

- [93] D. Wu, C. Zhu, M. Wu, H. Wang, J. Huang, D. Tang, J. Ma, Angew. Chem., Int. Ed. 2022, 61, 202315608.
- [94] J. Ma, M. Yu, M. Huang, Y. Wu, C. Fu, L. Dong, Z. Zhu, L. Zhang, Z. Zhang, X. Feng, H. Xiang, Small 2023, 20, 2305649.
- [95] Y. C. Liu, R. Jiang, H. F. Xiang, Z. M. Huang, Y. Yu, Electrochim. Acta. 2022, 425, 140746.
- [96] H. Z. Zhi, L. D. Xing, X. W. Zheng, K. Xu, W. S. Li, J. Phys. Chem. Lett. 2017, 8, 6048.
- [97] Y. Ji, Z. Zhang, M. Gao, Y. Li, M. J. McDonald, Y. Yang, J. Electrochem. Soc. 2015, 162, A774.
- [98] Y.-S. Kim, H. Lee, H.-K. Song, ACS Appl. Mater. Interfaces 2014, 6, 8913
- [99] X. N. Song, T. Meng, Y. M. Deng, A. M. Gao, J. M. Nan, D. Shu, F. Y. Yi, Electrochim. Acta. 2018, 281, 370.
- [100] X. Zheng, Z. Cao, Z. Gu, L. Huang, Z. Sun, T. Zhao, S. Yu, X.-L. Wu, W. Luo, Y. Huang, ACS Energy Lett. 2022, 7, 2032.
- [101] Y. Lin, X. Jin, S. Gao, F. Liu, S. Huang, X. Yang, Y. Chen, Y. Meng, Chemistry (Weinheim) 2024, 27, 16896.
- [102] X. H. Liu, J. H. Zhao, H. H. Dong, L. L. Zhang, H. Zhang, Y. Gao, X. Z. Zhou, L. H. Zhang, L. Li, Y. Liu, S. C. Chou, W. H. Lai, C. F. Zhang, S. L. Chou, Adv. Funct. Mater. 2024, 34, 2402310.
- [103] X. Z. Zhou, X. M. Chen, Z. Yang, X. H. Liu, Z. Q. Hao, S. Jin, L. H. Zhang, R. Wang, C. F. Zhang, L. Li, X. Tan, S. L. Chou, Adv. Funct. Mater. 2023, 34, 2302281.
- [104] J. Cai, W. Z. Fan, X. Q. Li, S. F. Li, W. L. Wang, J. P. Liao, T. X. Kang, J. M. Nan, Chem. Eng. J. 2024, 491, 151949.

- [105] J. Chen, Y. Peng, Y. Yin, M. Liu, Z. Fang, Y. Xie, B. Chen, Y. Cao, L. Xing, J. Huang, Y. Wang, X. Dong, Y. Xia, *Energy Environ. Sci.* 2022, 15, 3360.
- [106] E. M. Li, X. Tang, J. C. Zhou, H. M. Zhao, J. H. Teng, J. J. Huang, B. H. Dai, T. M. Lu, Q. D. Tao, K. B. Zhang, W. F. Deng, J. Li, *Chem. Eng. J.* 2024, 489, 151525.
- [107] I. Moeez, D. Susanto, W. Chang, H. D. Lim, K. Y. Chung, Chem. Eng. J. 2021, 425, 130547.
- [108] H. Lohani, A. Kumar, A. Bano, A. Ghosh, P. Kumari, A. Ahuja, A. Sengupta, D. Kumar, D. T. Major, S. Mitra, Adv. Energy Mater. 2024, 14, 2401268.
- [109] M. S. Park, J. Y. Choi, G. K. Veerasubramani, D. W. Kim, *Electrochem. Commun.* 2020, 119, 106829.
- [110] L. Madec, R. Petibon, K. Tasaki, J. Xia, J. P. Sun, I. G. Hill, J. R. Dahn, Phys. Chem. Chem. Phys. 2015, 17, 27062.
- [111] B. Zhang, M. Metzger, S. Solchenbach, M. Payne, S. Meini, H. A. Gasteiger, A. Garsuch, B. L. Lucht, J. Phys. Chem. C. 2015, 119, 11337
- [112] G. Yan, K. Reeves, D. Foix, Z. Li, C. Cometto, S. Mariyappan, M. Salanne, J.-M. Tarascon, Adv. Energy Mater. 2019, 9, 1901431.
- [113] Q. M. Zhang, Z. X. Wang, X. H. Li, H. J. Guo, W. J. Peng, J. X. Wang, G. C. Yan, J. Power Sources. 2022, 541, 231726.
- [114] O. Lavi, S. Luski, N. Shpigel, C. Menachem, Z. Pomerantz, Y. Elias, D. Aurbach, ACS Appl. Energy Mater. 2020, 3, 7485.
- [115] A. Nimkar, N. Shpigel, F. Malchik, S. Bublil, T. Fan, T. R. Penki, M. N. Tsubery, D. Aurbach, ACS Appl. Mater. Interfaces 2021, 13, 46478.



Kunchen Xie received his bachelor's degree from the School of Chemistry at Zhengzhou University (China) in 2023. He is currently pursuing a master's degree under the supervision of Prof. Feng Pan at the School of Advanced Materials, Peking University. His research interests are focused on the electrolytes for high-voltage lithium-ion batteries and sodium-ion batteries.



Yuchen Ji is currently a postdoctoral scholar in the Department of Mechanical Engineering at the University of Washington. He obtained his Ph.D. degree from Peking University in 2024. His research interests focus on interfacial evolution and in situ characterizations in secondary batteries.

16146840, 2025, 15, Downloaded from https://advanced.onlinelibrary.wiley.com/doi/10.1002/aemm.202405301 by University Town Of Shenzhen, Wiley Online Library on [17111/2025]. See the Terms

and Conditions

and-conditions) on Wiley Online Library for rules of use; OA articles are governed by the applicable Creative Commons



Luyi Yang received his bachelor's degree from the Department of Chemistry at Xiamen University (China) and earned PhD degree from the School of Chemistry at Southampton University (U.K.). He is currently an associate research professor at the School of Advanced Materials, Peking University, Shenzhen Graduate School. His research interests mainly focus on exploring the interfacial reaction processes and failure mechanisms of lithium-ion batteries and designing corresponding improvement strategies.



Feng Pan, chair professor of Peking University, Vice President of Shenzhen Graduate School of Peking University, Founding Dean of the School of New Materials, Member of the Chinese Chemical Society, and executive editor of Structural Chemistry. He has long been committed to the development of structural chemistry methodology and its application in the research and development of new materials, created the structural chemistry theory based on graph theory, established the in situ dynamic structure characterization system based on large scientific devices such as neutron and synchrotron radiation, and explored and revealed the material genes and structure-function relationship. Breakthroughs have been made in solving scientific problems such as lithium battery energy storage density, power density, and stability. He has published more than 430 SCI articles in well-known journals such as Nature (2), Nature Energy (1), and Nature Nanotechnology (3) as the corresponding author. He has been awarded the China Electrochemical Contribution Award and the Battery Technology Award of the American Electrochemical Society.